Biogeosciences, 23, 5477–5495, 2026
https://doi.org/10.5194/bg-23-5477-2026

Biogeosciences Open Access EGU

Planktonic foraminifera iodine / calcium ratio: is it a proxy for dissolved oxygen in the ocean?

Vincent Guarinos[1], Kazuyo Tachikawa[1], Marta Garcia[1], Giuseppe Siani[2], Marie Revel[3], Hartmut Schulz[4], Francisco Sierro[5], and Thomas Chalk[1]

[1]Aix Marseille Univ, CNRS, IRD, INRAE, Coll France, CEREGE, Aix-en-Provence, France
[2]Laboratoire de Géosciences Paris-Saclay (GEOPS), CNRS, Paris Saclay, France
[3]Université de la Cote d'Azur, CNRS, OCA, IRD, Geoazur, Valbonne, France
[4]Department of Geosciences, University of Tübingen, Tübingen, Germany
[5]Dept. de Geología, Univ. de Salamanca, Plaza de los Caídos s/n, 37008, Salamanca, Spain

Correspondence: Vincent Guarinos (guarinos@cerege.fr)

Received: 2 February 2026 – Discussion started: 12 February 2026
Revised: 24 July 2026 – Accepted: 27 July 2026 – Published: 10 August 2026

Abstract. Direct observations indicate a declining trend in ocean oxygen concentrations, which is not quantitatively captured by models. The complexity of oxygenation variability, linked to both physical and biochemical parameters, must be investigated across different modern climate contexts. Foraminiferal iodine-to-calcium (I / Ca) ratios have emerged as a proxy for subsurface oxygen concentrations although their capacity for quantitative reconstructions remains to be elucidated. We provide a new database of modern foraminiferal I / Ca, including the first results from the Mediterranean Sea and new samples in the Arabian Sea together with the parameters of biochemistry (nutrient concentration, pH, chlorophyll, oxygen, net primary productivity), physical and geographical (temperature, salinity, latitude, distance from the coast, water depths) and diagenesis potential (depth in core, sediment age) to better understand the proxy behaviour. Considering the strong spatiotemporal variability in dissolved oxygen in subsurface ocean, we propose to use statistically robust 25th percentile of oxygen concentration (p25 [O_2]) in the upper 500 m in the water column instead of minimum concentration. Our results affirm that oxygen concentration is the primary driver of foraminiferal I / Ca and we propose a new calibration equation of foraminiferal I / Ca against p25 [O_2]. Based on a new database, we identify a complex relationship between p25 [O_2] and iodine speciation, which is one of the main sources of scatter. A comparison with synthetic calcite reveals that planktonic foraminiferal tests can incorporate either more or less iodate at high p25 [O_2] than abiotic calcite, probably due to "vital effects". The Mediterranean Sea samples present a wide range from low to high I / Ca (0.6 to 6.9 µmol mol^{-1}) in well-oxygenated water, which cannot be explained solely by authigenic calcite precipitation. Our results highlight the complex behaviour of the I / Ca proxy, while its semi-quantitative reconstruction in palaeoceanography remains promising.

1 Introduction

Oxygen concentration [O_2] in the global ocean is decreasing, and the decline is highly influenced by warming patterns induced by global climate change (Oschlies et al., 2018). Future oxygenation change is difficult to predict as it depends on various parameters. Dissolved oxygen depletion can be related to changes in solubility with seawater temperature, generally decreasing ventilation of water masses (Oschlies et al., 2017), and through biological productivity triggered oxygen consumption in the ocean, especially in the subsurface, where the productivity and remineralisation are at a maximum. Models can currently only explain about half the observed oxygen depletion (Bopp et al., 2013; Frölicher et al., 2016) and thus a proxy for subsurface oxygen content is highly sought to study longer variability under different climate conditions.

Published by Copernicus Publications on behalf of the European Geosciences Union.

The iodine to calcium ratios (I / Ca) from planktonic foraminifera tests have been investigated and used as a proxy for subsurface/intermediate depth minimum oxygen concentration (Lu et al., 2010, 2016, 2020; Winkelbauer et al., 2021; Hess et al., 2025; Zhou et al., 2014, 2022; Hoogakker et al., 2025) as inorganic iodine speciation depends on redox potential, which is mainly controlled by oxygen content (Luther, 2023). Severe oxygen depletion, less than 1 nM of oxygen, will chemo-dynamically trigger iodate reduction to iodide (I^-) (Luther, 2023). In oxygenated water, iodine is mainly in its oxidized form, iodate (IO_3^-) (Chance et al., 2014, 2019). Iodide, the reduced form of inorganic iodine can also be found in small concentrations near surface because of biological iodate uptake and iodide release during phytoplankton growth (Hepach et al., 2020). In hypoxic and anoxic waters, iodide is the major iodine species, thought to increase as iodate is reduced. The reduction reaction takes place under short time scales, from days to weeks (Chance et al., 2010) whereas the full (re)oxidation of iodide back to iodate has been reported to take place from several weeks to several months (Wadley et al., 2020). Total inorganic iodine in oxygenated water typically ranges between 400 and 500 nM, corresponding to a variability of about 20 % (Chance et al., 2010). Iodine is also present as organically bound iodine, primarily in the form of dissolved organic iodine. In the open ocean, it is typically about 5 % of total dissolved iodine, but this proportion can increase to up to ~ 20 % in coastal areas due to interaction with higher concentrations of dissolved organic matter (Jones et al., 2024). Iodate is assumed to be the only iodine species to be incorporated to foraminiferal calcite tests as a substitute to carbonate ion (Feng and Redfern, 2018; Lu et al., 2010; Podder et al., 2017). The processes and kinetics of the chemical reactions in the water column, as well as its incorporation mechanisms into biologically mediated calcite are still poorly understood (Luther, 2023).

Calibration of the I / Ca–O_2 proxy was first focused on the quantitative reconstruction of subsurface oxygen concentration as synthetic calcite showed linear incorporation of iodate depending on its concentration (Lu et al., 2010). Later, foraminiferal core-top calibrations started to relate the I / Ca ratio in respect with minimum oxygen from 0–500 m in the water column, considering a tight relationship between the minimum oxygen concentration and surface water iodate concentration (Lu et al., 2016). The proxy was thus proposed as a semi-quantitative tool with thresholds I / Ca value of 0.85 2.3 and 5 µmol mol^{-1} that corresponds to [O_2] 50, 90 and 140 µmol kg^{-1} (Lu et al., 2016; Wang et al., 2026). Data from the Southeast Atlantic including sites close to the Benguela upwelling system highlighted the possibility of low I / Ca in apparently oxygenated water (Lu et al., 2020). The minimum oxygen values of the study region were highly spatially variable and the use of oxygen data at higher resolution (0.25°) reduced the number data points with low I / Ca under high oxygenation condition (Lu et al., 2020). However, substantial scatter remains in the relationship between foraminiferal I / Ca and minimum oxygen concentration that is characterised by two broad domains: oxygen depleted waters (I / Ca < 2.5 µmol mol^{-1}) and oxygenated water (I / Ca > 4 µmol mol^{-1}). Nilsson-Kerr et al. (2025) expanded the I / Ca–O_2 core top calibration dataset with measurements from regions with low subsurface O_2, confirming the presence of significant scatter. Hess et al. (2025) proposed that I / Ca dispersion is linked with the different iodate concentrations at different foraminiferal calcification depths. Scattering could then be reduced by using Mg / Ca ratios in the foraminifera, a proxy for temperature that estimates their calcification depth. Although they showed that I / Ca varies predictably based on iodate concentration and water depth, substantial dispersion still persists and the effect of calcification depth cannot explain all the results.

Moreover, low I / Ca from plankton tow in highly oxygenated waters have been measured (Winkelbauer et al., 2023). It was suggested that iodine is incorporated during particle sinking and could explain those low values, thus challenging the use of the proxy for subsurface oxygenation, an interpretation that has not yet been further interrogated. Besides, given the lack of knowledge on the underlying mechanism, application of this proxy needs caveating when carried out for samples from coastal shelves and restricted basins where the mixing with open ocean water is not efficient (Hess et al., 2025; Lu et al., 2020).

The previous studies have mostly focused on trying to reduce scattering by investigating the y-axis (I / Ca), but the definition of x-axis (oxygen concentration) has not been treated systematically, despite its importance (Lu et al., 2020). Some studies suggest that the complexity of iodine speciation and its coupling with dissolved oxygen is responsible for the observed data scatter (Hess et al., 2025; Nilsson-Kerr et al., 2025). However, the systematic study with a large number of data focusing on both the definition of minimum dissolved oxygen concentration and iodine speciation has not yet been realised.

We aim to determine whether the definition of "oxygen concentration" can help to better calibrate the proxy, and further investigate the possible reasons for foraminiferal I / Ca data scattering. We also examine if the proxy can be used in a semi-enclosed basin, the Mediterranean Sea as important oceanographical variations over small distances may limit the use of the proxy (Hess et al., 2025). In this paper, our approach is to (1) propose a statistically robust definition for minimum O_2, (2) investigate the coupling between iodine speciation and dissolved oxygen as a potential control for foraminiferal I / Ca scattering (3) examine the differences in iodine incorporation between foraminiferal and abiotic calcite, and (4) evaluate the influence of authigenic carbonate precipitation on foraminiferal I / Ca under high alkalinity conditions.

2 Material and Methods

2.1 Material

In this study we present core top planktonic foraminiferal I / Ca from 7 locations including 5 from the Mediterranean region (Fig. 1b). Core MD99-2341 (577 m b.s.l.) from Gulf of Cadiz together with ODP Site 977 (1984 m b.s.l.) from Alboran Sea are selected to characterise the Atlantic inflow signature. MD04-2797 (771 m b.s.l.) is located next to the Strait of Sicily, and is used to indicate mixing ratio at the connection between the Western and Eastern Mediterranean basins. SL95 (1390 m b.s.l.), in the Gulf of Sirte, is thought to represent the southern part of the Ionian Sea. Core MD04-2724 (1659 m b.s.l.) has been recovered in the deep Nile delta and it is the easternmost core of this study. Core MD04-2722 (1780 m b.s.l.) was recovered in the Levantine basin. MD90-917 (1010 m b.s.l.), was recovered in the Adriatic Sea, where the Eastern Mediterranean deep water is formed and corresponds to a well oxygenated area. The two other cores MD04-2873 (2196 m b.s.l.) and MD04-2876 (828 m b.s.l.) were recovered in the Pakistan margin, one below the Oxygen Minimum Zone (OMZ), and the other inside it, respectively (Fig. 1c). They are selected in order to identify any impact of the bottom water oxygenation state on I / Ca ratios.

The core top materials of the two new cores, SL95 and MD04-2724, were dated to 1835 ± 30 (1 SD, at 0–1 cm) and 5515 ± 30 radiocarbon years BP (1 SD, at 0–1 cm) respectively, using mono-species planktonic foraminifera performed at the ARTEMIS facility in Gif-sur-Yvette, France.

2.2 Analysis of iodine / calcium ratio from planktonic foraminifera

For foraminiferal I / Ca analysis, 30 monospecific planktonic foraminiferal tests were picked from 250–355 µm fraction and cleaned following Barker et al. (2003) short-cleaning protocol. Only the oxidative cleaning was realised. Depending on the core, different species are used. For Gulf of Cadiz, *Globigerinoides ruber albus* (hereafter referred to as *G. ruber*), *Globigerina bulloides*, *Trilobatus sacculifer* (without sack-like chamber), *Globigerinella siphonifera* and *Pulleniatina obliquiloculata* were picked. Given the influence of calcification depth on I / Ca ratios (Hess et al., 2025), species-specific calcification depths are reported here. *Globigerinoides ruber* and *T. sacculifer* are mixed layer calcifiers. *G. bulloides*, *G. siphonifera* and *P. obliquiloculata* are thermocline-dwelling species. For the Alboran Sea, *G. ruber* and *G. bulloides* ratios were analysed. For MD04-2797, SL95, MD90-917 and the two cores from the Arabian Sea, only *G. ruber* was used. After cleaning, samples were dissolved with diluted nitric acid at 0.1 M (0.66 %). The obtained solution was then centrifuged to separate any residual non-dissolved particles. After a calcium (Ca) concentration test to determine the necessary dilution factor for each sample, an aliquot for iodine measurement is stabilised with tetramethylammonium hydroxide (TMAH, SIGMA-ALDRICH) to obtain a 0.33 % HNO_3^- 0.48 % TMAH matrix. The solution is then diluted to a Ca concentration of 50 µg mL^{-1} (50 ppm). The remainder is diluted to obtain Ca concentration of 100 µg mL^{-1} to determine Ca, U, Mn, Fe and Al concentrations (Guarinos et al., 2026b). In this study only I / Ca ratio is discussed. Elemental analysis is carried out using ICP-MS (Agilent 7500ce) at the CEREGE, France.

Each sample is analysed and standard-sample bracketing is used to characterise instrumental drift during measurement. There is no currently certified geostandard for I / Ca but JCp-1, a coral powder, is commonly used in this role. In our analyses JCp-1 is measured every five samples. Our measure of I / Ca of JCp-1 is 4.34 ± 0.11 µmol mol^{-1} ($n = 27$, 1 SD). This is in good agreement with published values of 4.27 ± 0.10 µmol mol^{-1} ($n = 13$, 1 SD, Winkelbauer et al., 2023), 4.33 ± 0.06 µmol mol^{-1} ($n = 6$, 1 SD, Chai and Muramatsu, 2007), 4.27 ± 0.06 µmol mol^{-1} (1 SD, Lu et al., 2010), and 4.20 ± 0.43 µmol mol^{-1} (1 SD, Hess et al., 2025). Calculated I / Ca precision is better than 3 % and blank levels were low, often below detection limits, so no correction is applied.

2.3 Inorganic iodine speciation depending on dissolved oxygen concentration

The concentration of inorganic iodine species in the ocean is primarily controlled by redox conditions, with iodate prevailing in oxic conditions and iodide dominating in reducing environments (Chance et al., 2014; Ullman et al., 1990). To establish the relationship between iodate and oxygen concentration, iodine data are expressed as iodate proportion in total inorganic iodine in order to avoid potential impacts from changing iodine concentration. We have selected data shallower than 500 m b.s.l. and within $\pm 1\sigma$ of total inorganic iodine concentration (Fig. 3c) to avoid heavily iodine enriched/depleted areas. Only data with both iodate and iodide concentrations are selected to better constrain the speciation and avoid assumption on total inorganic iodine concentration. Iodine speciation data from Bermuda inshore water are excluded (Jickells et al., 1988), as they originate from a highly restricted environment, and not representative of the conditions considered in this study. Data analysis is performed using least-squares fitting analysis in Python 3.12. The 95 % prediction intervals are computed by propagating the uncertainties of the fitted model parameters contained in the covariance matrix. This combines both the variance of the fitted parameters and the residual variance of the data within the selected area.

To explore the influence of redox conditions on inorganic iodine speciation, oxygen data were combined with published iodine speciation measures. Inorganic iodine speciation in the upper 500 m is investigated using previously

Table 1. Description of cores and planktonic foraminiferal species used for I / Ca analysis. NA is for non attributed.

Core name	Location	Latitude	Longitude	Depth (m b.s.l.)	Depth in core (cm)	Core top age (ka cal BP)	Species picked	Comment	Age model reference
MD99-2341	Gulf of Cadiz	36.383	−7.533	577	2–4	1.02	*G. ruber, G. bulloides, T. sacculifer, G. siphonifera, P. obliquiloculata*	Atlantic water inflow	Eynaud et al. (2009)
ODP Site 977	Alboran Sea	36.032	−1.955	1984	23–25	1.37	*G. ruber and G. bulloides*	Atlantic water inflow	Martrat et al. (2004)
MD04-2797	Sicily Strait	36.959	11.666	771	0–1	0.70	*G. ruber*	Connection between basins	Cornuault et al. (2018)
SL95	Gulf of Sirte	32.774	19.191	1390	0–1	1.20	*G. ruber*	South Ionian Sea	This study
MD04-2724	Levantine Sea	33.033	29.150	1659	5–6	6.00	*G. ruber, T. sacculifer*	Deep Nile delta	This study
MD04-2722	Levantine Sea	33.100	33.500	1780	0–1	3.60	*G. ruber*	Eastern basin edge	Cornuault et al. (2018)
MD90-917	Adriatic Sea	41.280	17.620	1010	2–3	0.65	*G. ruber*	Well oxygenated	Siani et al. (2010)
MD04-2873	Pakistan Margin	23.532	63.827	2196	1–2	*NA*	*G. ruber*	Below the OMZ	Pichevin et al. (2007)
MD04-2876	Pakistan Margin	24.849	64.014	828	2–3	*NA*	*G. ruber*	Within the OMZ	Bard et al. (2013)

published data (Winkelbauer et al., 2023). Oxygen concentrations were obtained from World Ocean Database 2023 (WOD23) from Mishonov et al. (2024) from within a 0.25° area around each sampling site, where possible. From every obtained oxygen distribution, we determined the percentiles of oxygen concentration. Each measurement from 0–500 m at a given station is attributed to the same percentile value.

2.4 Planktonic foraminiferal I / Ca database

Planktonic foraminiferal I / Ca database is obtained with 15 new core top data (this study), and previously published core top and plankton tow measurements (Hess et al., 2025; Lu et al., 2020, 2016; Nilsson-Kerr et al., 2025; Winkelbauer et al., 2021, 2023; Zhou et al., 2022).

The database contains 567 core top data points, 438 of which are younger than 2,000 years BP. Oxygen distribution in the first 500 m are obtained from WOD23 accepted values (class 0) from (i) Bottle (Winkler titration) and (ii) Conductivity–Temperature–Depth (CTD) with oxygen sensor data in a 0.25° area around each sampling site (Mishonov et al., 2024). For sites where no oxygen profile is available, the area of search is extended to 0.5° and the data flagged, no data from $> 0.5°$ is used. The obtained oxygen concentration data are used to calculate the minimum, maximum, mean, and percentile values. CTD measurements are only used for 3 I / Ca values as they are considered to be less accurate because of excursion artifacts. For this reason, we prioritise bottle data which are consider to be more accurate.

Additional environmental variables are included to assess their potential contribution to I / Ca variability. Other parameters, seawater temperature, salinity, nitrate, phosphate, chlorophyll, pH and alkalinity are similarly obtained from class 0 bottle measurements in 0.25° around sampling site at the first 500 m. Investigating the 0–500 m is crucial because this is where the planktonic I / Ca signal is presumed to originate (Lu et al., 2016). Oxycline depth and mean oxygen concentration at oxycline were also tested as they may highly influence foraminiferal I / Ca (Wang et al., 2026). They were recovered from class 0 bottle measurements in 0.25° area around sampling site. No value is attributed to sites without any available bottle measurement. Other parameters, net primary productivity (NPP) (Behrenfeld and Falkowski, 1997; ORCA Science, 2025), current speed, and mixed layer depth, are obtained using their corresponding raster resolution. NPP is derived from annual mean satellite data integrated from 1998 to 2022 at a resolution of 25 km and using Eppley-Vertically Generalized Production Model (Eppley-VGPM). Parameters related to ocean dynamics are derived from Global Ocean Physics Reanalysis annual mean and maximum values (Lellouche et al., 2021). We use absolute Northward and Eastward velocities from surface to 500 m and mixed layer depth. Data sources are listed in Table 2.

The database construction we propose here is a table format with two entries. Each line is a specific measurement of foraminiferal I / Ca. Columns correspond to different characteristics of the measurement, sampling site, and all the extracted site-specific parameters previously mentioned. Information of symbionts presence and habitat depth is also shown. We also specify the cleaning protocol of the samples as reductive cleaning has been shown to reduce the I / Ca value by 30 % (Zhou et al., 2022). Samples processed by reductive cleaning are corrected accordingly, with an increase of 30 % of I / Ca. This impacts 197 measures (35 % of the full dataset). All the figures presented are using the corrected I / Ca. The full database is available in Supplement.

To assess the relationships between foraminiferal I / Ca and environmental variables, we use both Spearman's ρ and Kendall's τ correlation coefficients. Even if some individual uncertainties of the selected variables may follow normal distributions, the dataset as a whole is heterogeneous and non-normally distributed, making non-parametric tests more appropriate. Moreover, as the resulting relationships are likely non-linear, these rank-based methods provide a robust evaluation of correlation. The use of both correlation coefficients captures two complementary aspects of monotonic relation-

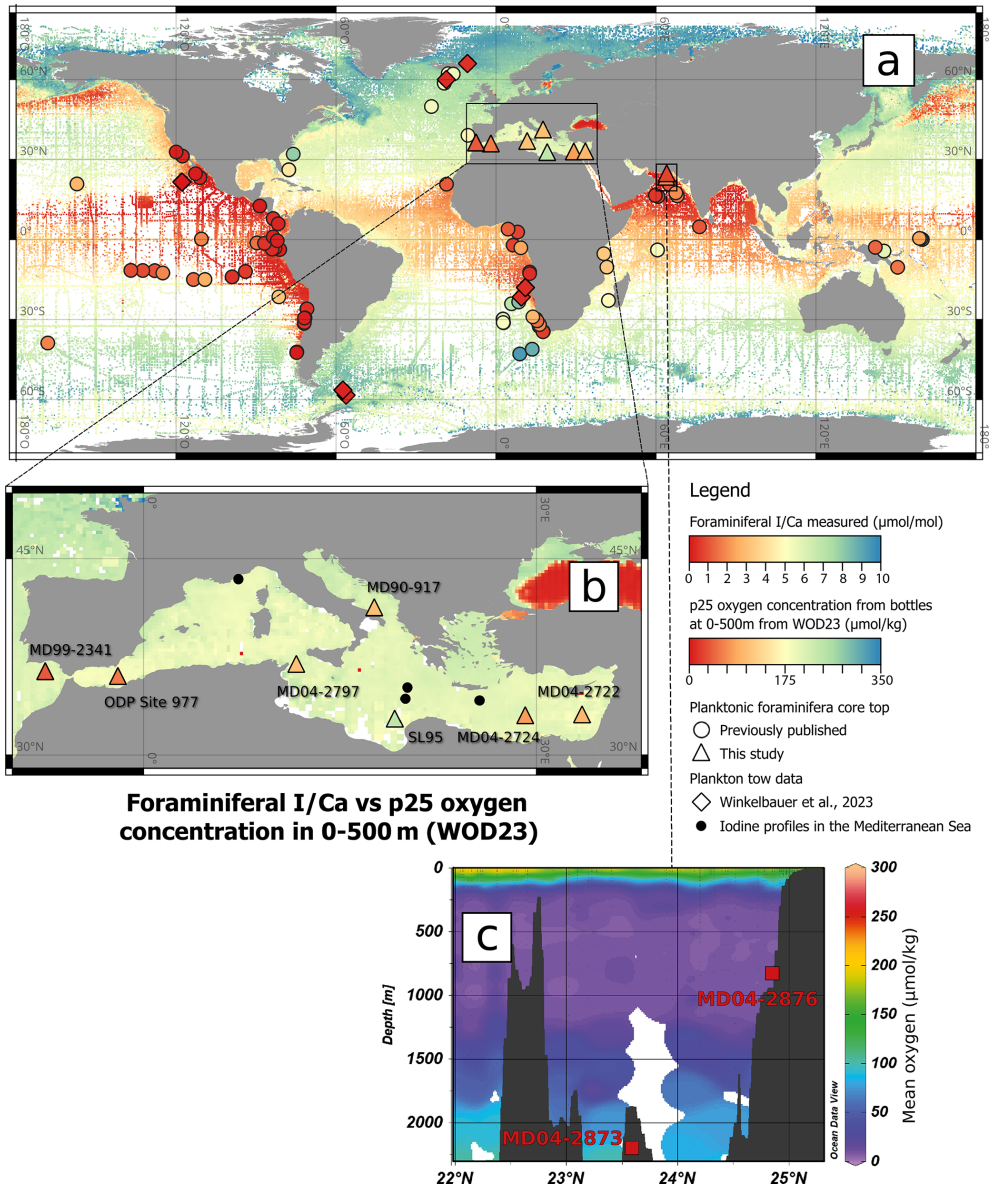

Figure 1. Map of 25th percentile of oxygen concentration (p25 [O_2]) in µmol kg^{-1} in ±0.25° (latitude and longitude) at 0–500 m b.s.l. and symbols corresponding to modern foraminiferal I / Ca (µmol mol^{-1}) less than 8000 years (8 ka) before present (BP) at global scale **(a)** and in the Mediterranean Sea **(b)**. The locations of new core top data from this study are represented with triangles and published values with circles. Plankton tow data from Winkelbauer et al. (2023) are represented with diamonds. Position of dissolved inorganic iodine species concentrations in the Mediterranean Sea are represented in black (Tian and Nicolas, 1995; Ullman et al., 1990). Oxygen distributions were obtained from World Ocean Database 2023 (WOD23) (Mishonov et al., 2024). Arabian Sea mean oxygen section **(c)** shows the position of the two core-tops studied. MD04-2876 is in the core of the OMZ, and MD04-2873 is below. Oxygen profile is made with Ocean Data View (Ocean Data View, 2025).

ships: the strength of the association and how well the observations agree with each other. These analyses are intended to identify statistical covariation.

3 Results

3.1 Definition of p25 [O_2] and Iodine speciation

Oxygen concentration ranges from 0 to 300 µmol kg^{-1}. Obtained oxygen distribution in the upper 500 m layer at sites where foraminiferal I / Ca is available are mostly unimodal or multimodal (Fig. 2). Previous studies use the minimum

$[O_2]$ value measured in 0–500 m to calibrate foraminiferal I / Ca (Hess et al., 2025; Lu et al., 2020). The use of the minimum value can provide questionable representativeness of actual conditions because the minimum value could reflect exceptional events or data reporting issues. As the distribution of oxygen concentration at 0 to 500 m water depth is not normally distributed, we use the 25th percentile (p25) to represent average oxygen depletion instead of the minimum value. Its use is thought to partially eliminate outliers or errors in the oxygen dataset. The use of percentiles takes into account the full distribution in 0–500 m in space and time as much as the oxygen dataset allows. However, this indicator is not perfect as important errors or sampling bias may still influence the values. Furthermore, the goal of the use of p25 is not to propose a quantitative interpretation of the proxy. Iodine concentration and speciation dynamics may not be fully captured by oxygen variability and result in subsequent dispersion. We have tested percentiles from 5 to 30 at each 5 % (Fig. S1 in the Supplement). All tested definition of x-axis shows the same slope, with only the intercept being different. We choose the higher R^2 (0.43) together with the lower Root Mean Square Error (RMSE) (1.370), corresponding to p25 (Fig. S1). We note here that p25 value is close to mean value minus 1 standard deviation when the distribution was normal or quasi-normal. With p25 being the oxygen parameter with the best fit, it is possible to remove part of the oxygen influence on the proxy.

In strongly oxygen-depleted areas, such as OMZ, the oxygen distributions are mainly multimodal with high values near surface and lower values in the heart of OMZ (Fig. 2a). Those areas are represented with p25 $[O_2]$ values ranging from 0 to 100 µmol kg^{-1}.

In areas with p25 $[O_2]$ value between 100 and 180 µmol kg^{-1} (tropical Atlantic Ocean, Ontong Java Plateau in the tropical Pacific), the distribution of oxygen concentration is mostly multimodal, reflecting vertical change with water depth but with moderate oxygen depletion (Fig. 2b).

Oxygenated waters are marked by p25 $[O_2]$ values from 180 to 300 µmol kg^{-1}. The corresponding distributions are mostly unimodal (Fig. 2c). Some sites were not attributed to a distribution type due to their relative rarity.

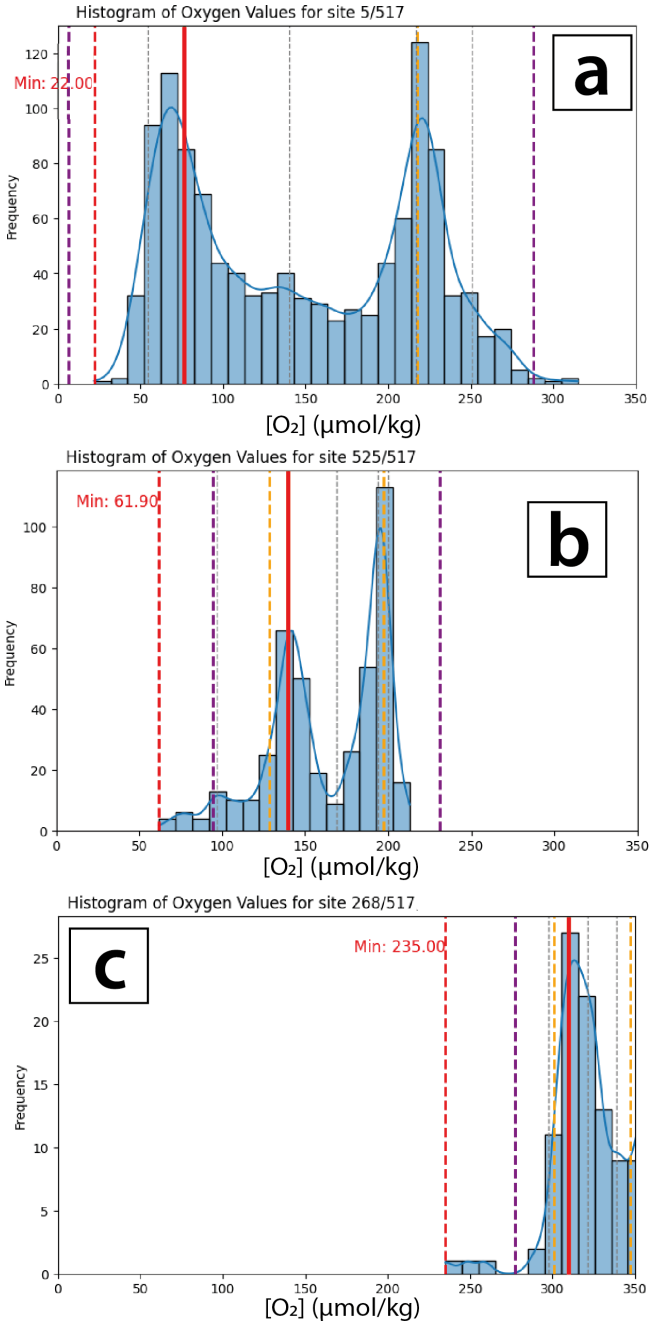

Figure 2. Histograms of common types of oxygen distributions encountered in this study, with OMZ-type from Mauritanian upwelling **(a)**, intermediate from southwestern Pacific Ocean **(b)** and well oxygenated from North Atlantic **(c)** distributions. Oxygen depletion representative value p25 $[O_2]$ is highlighted in full red line. Other percentiles (p5, p50, p75, p95) are in dotted grey lines. Dotted red line is the minimum oxygen value previously used. Dotted yellow and purple lines are 1σ (68 %) and 2 σ (95 %) limits, respectively. The difference between $[O_2]$ min and p25 $[O_2]$ is 0–142 µmol kg^{-1}. Note that the shown oxygen concentration range is different between **(a)**, **(b)** and **(c)**.

3.2 Iodine speciation and oxygen concentration

Total inorganic iodine is in the range of 400 to 500 nM and is more or less constant in the ocean (Chance et al., 2010) (Fig. 3c). Inorganic iodine depletion near coastal regions have been attributed to biological uptake (Elderfield and Truesdale, 1980; Wong and Zhang, 1992). But inorganic iodine speciation primarily varies with redox potential, largely governed by oxygen availability (Luther, 2023). In order to compare inorganic iodine speciation to foraminiferal I / Ca, we represent it from the first 500 m as a function of p25 $[O_2]$ in 0–500 m (Fig. 3a) and $[O_2]$min in 0–500 m. Speciation is shown as iodate/(iodate + iodide) in Fig. 3a, that

corresponds to the iodate proportion of the inorganic iodine concentration (Tian and Nicolas, 1995). This representation allows us to minimise the effect of inorganic iodine concentration (Elderfield and Truesdale, 1980; Tian and Nicolas, 1995). As this approach is based on real data, it may partly account for other factors affecting inorganic iodine speciation such as mixing of water masses and primary productivity (Cheng et al., 2024; Evans et al., 2020; Hardisty et al., 2021; Moriyasu et al., 2020). The aim of Fig. 3 is not to compare the two x-axes, but rather to present a different concept for inorganic iodine speciation (Fig. 3a) than the common iodate concentration (Fig. 3b). This is especially visible with samples from the Indian Ocean with lower iodate concentration than the other oceans (Fig. 3b) being in the cloud of points with inorganic iodine speciation (Fig. 3a) (Chance et al., 2020; Farrenkopf and Luther, 2002).

Main result shows high dispersion of iodine speciation, and non-linear relationship (Fig. 3a and b). It also shows that iodate might exist in oxygen depleted waters, especially in Pacific Ocean. Iodine speciation is highly variable at 0–500 m. Iodate absence is mainly found at p25 [O_2] $< 10\,\mu mol\,kg^{-1}$ although it is not systematically absent in those areas. In well oxygenated water ($>200\,\mu mol\,kg^{-1}$), inorganic iodine is principally under the oxidised form, with a proportion above 60 %. However, measurements from one site in Pacific and three in Atlantic are low in iodate proportions (< 0.5) in oxygenated areas ($> 150\,\mu mol\,kg^{-1}$), and fall outside the prediction interval.

We choose an exponential fit function to represent the rapid iodate decrease when p25 [O_2] is below $20\,\mu mol\,kg^{-1}$ and the plateau in oxygenated waters (p25 [O_2] $>180\,\mu mol\,kg^{-1}$) (Fig. 3a). Prediction interval for exponential fit is represented in shaded red area. The objective of this representation is not to find the best fit, but rather to determine whether the relationship between iodate proportion and dissolved oxygen content could explain the variation in foraminiferal I / Ca-based oxygen reconstruction. Compared to min[O_2] and iodate concentration (Fig. 3b), the use of p25 [O_2] with proportion of iodate in inorganic iodine (Fig. 3a) limits the influence of total inorganic iodine concentration change. The main difference in the x-axis definition is the change in range, from 0–$280\,\mu mol\,kg^{-1}$ for [O_2] min to 0–$330\,\mu mol\,kg^{-1}$ for p25 [O_2] (Fig. 3a, b). This results in a visually stretched dataset in the x-direction. Moreover, the use of a different y-axis leads to fewer values outside the 95 % prediction interval in the high-iodate-proportion/low-p25 range compared to iodate concentration. A few points fall below the 95 % prediction interval at intermediate oxygen levels when using p25 [O_2].

In the Mediterranean Sea, inorganic iodine speciation profiles are scarce, with only one time series and four different locations reported (Tian and Nicolas, 1995; Ullman et al., 1990). Nevertheless, consistently high iodate concentrations are observed in the upper 0–500 m (370–515 nM) corresponding to well oxygenated water ([O_2]min 100–$180\,\mu mol\,kg^{-1}$) (Fig. 3b). Under these conditions, iodate represents more than 80 % of total inorganic iodine, with p25 [O_2] between 190 and $200\,\mu mol\,kg^{-1}$.

3.3 New core top planktonic foraminiferal I / Ca

Low iodine concentration in foraminifera, ranging from 0 to $2\,\mu mol\,mol^{-1}$, are mostly found with p25 [O_2] between 0 and $180\,\mu mol\,kg^{-1}$ (Fig. 4). In the 180–$300\,\mu mol\,kg^{-1}$ of p25 [O_2], most foraminiferal I / Ca ratios show higher values ranging from 1 to $8\,\mu mol\,kg^{-1}$.

New core top data from the Pakistan margin present I / Ca values lower than $2.5\,\mu mol\,mol^{-1}$ ($0.7\,\mu mol\,mol^{-1}$ for MD04-2876 and $1.8\,\mu mol\,mol^{-1}$ for MD04-2873). Difference in p25 [O_2] could be related to oxygen data availability with wider area of oxygen distribution of 0.5° for MD04-2873 instead of 0.25° for MD04-2876 and different number of oxygen profiles ($n = 2$ and $n = 7$ respectively).

In the Mediterranean Sea, foraminiferal I / Ca values are very low in highly oxygenated areas ($1.0\,\mu mol\,mol^{-1}$ in the Gulf of Cadiz and 1.6 to $3.1\,\mu mol\,mol^{-1}$ in Alboran Sea) that corresponds to p25 [O_2] between 180 and $220\,\mu mol\,kg^{-1}$ (Fig. 4), or 168 and $190\,\mu mol\,kg^{-1}$ for min[O_2]. The observed trend cannot be explained by vertical oxygen structure or by seasonal oxygen-depletion events, as dissolved oxygen profiles in the upper 500 m show very limited seasonal or inter-annual variability, even when more than 20 profiles per site are considered. Regarding I / Ca difference between planktonic foraminiferal species, three cores provide information (Table 1). The dispersion of different species of foraminifera is around 40 % for the Gulf of Cadiz (MD99-2341) and the Alboran Sea (ODP Site 977) whereas in the Eastern Mediterranean Sea the high I / Ca ratios (from 2 to $6\,\mu mol\,mol^{-1}$) are associated with a dispersion of 50 % for the deep Nile Delta core (MD04-2724).

Iodine incorporation during particle sinking has been proposed to explain the low I / Ca values from plankton tows (Winkelbauer et al., 2023). However, we find no systematic relation with water depth and I / Ca with our new data (Fig. 4). Deep sites in oxygenated water like ODP Site 977 at 1984 m b.s.l. also show very low I / Ca. Other cores at comparable depths and oxygenation levels, like MD04-2724 at 1659 m b.s.l. show I / Ca above $4\,\mu mol\,mol^{-1}$.

3.4 Planktonic I / Ca values and the environmental parameters on global scale

The relationship between environmental parameters such as biogeochemical characterisation of 0–500 m at each site, primary productivity and physical parameters (current velocity) and foraminiferal I / Ca is investigated using statistical test Kendall's τ and Spearman's ρ correlation coefficients (Table 2). We only include samples more recent than 2 ka BP in the statistical analysis because older samples are less likely

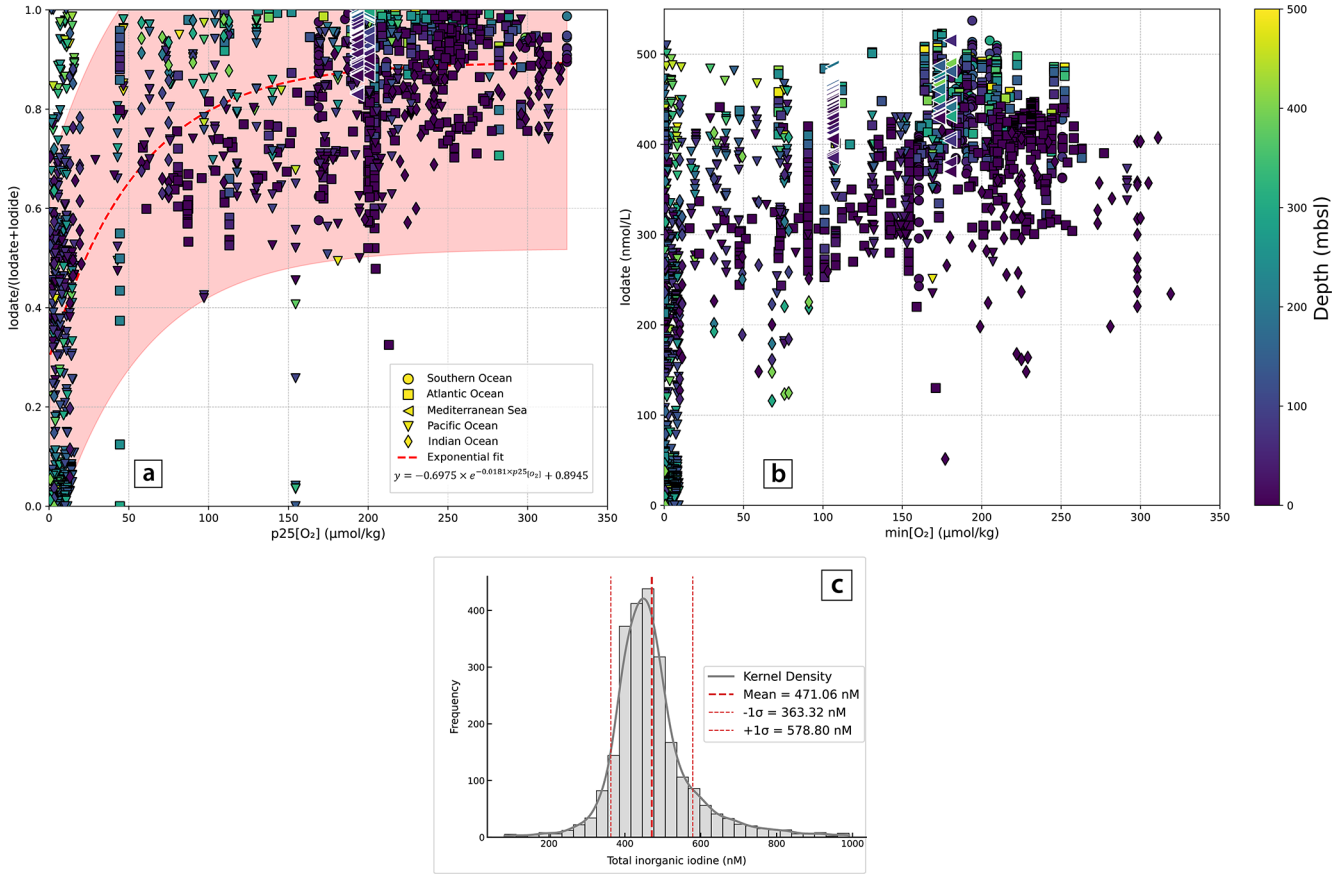

Figure 3. Iodate proportion in total inorganic iodine, iodate/(iodate + iodide) in 0–500 m as a function of p25 **(a)** (Spearman $\rho = 0.625$, Kendall $\tau = 0.447$, p-values < 0.01) and iodate concentration as a function of minimum **(b)** (Spearman $\rho = 0.650$, Kendall $\tau = 0.470$, p-values < 0.01) $[O_2]$ (µmol kg^{-1}) at 0–500 m. The proportion of iodate in inorganic iodine was obtained from Winkelbauer et al. (2023) and are classified by ocean. Mediterranean sites are highlighted with white contour. Red dotted line is the exponential fit of this relation ($y = -0.6975 \cdot \exp(-0.0181 \cdot x) + 0.8945$ for p25), with the 95 % prediction interval filled in red. Total inorganic iodine distribution with mean and $\pm 1\sigma$ values **(c)**.

to be representative of modern conditions. The results are reported in Table 2.

All oxygen related variables (minimum, maximum, mean, p25, oxycline mean oxygen concentration, mean (all depths) and bottom mean oxygen) are significantly linked to foraminiferal I / Ca with coefficients above 0.6 and 0.4 for Spearman's ρ and Kendall's τ, respectively, and p-values less than 0.01 for both cases (Table 2). Mixed layer depth and mean phosphate concentration show high correlation coefficients, but these parameters are also tightly linked to oxygen (Fig. S2). This observation supports an oxygen control on foraminiferal I / Ca, although the quantitative relationship remains uncertain.

Minimum pH, alkalinity, mean nitrate concentration and NPP present correlation with I / Ca (Table 2) but they also covary with p25 $[O_2]$ and are thus not independent (Fig. S2). Distance to coast, mean salinity, latitude and current velocity also show significant correlations with foraminiferal I / Ca. However, their correlation coefficients are less than half those of the strongest correlations identified. These variables are therefore not further discussed as primary drivers of foraminiferal I / Ca variability. He et al. (2026) documented a latitudinal trend in I / Ca that mirrored the iodate/latitude relationship. Similar pattern is found with I / Ca in Fig. S5. However, p25 $[O_2]$ also shows very similar trend with latitude with the two variables being correlated. It is also plausible that the temperature gradient at different latitudes controls the solubility of dissolved oxygen. Considering only temperature change from 8 to 28 °C at a constant salinity of 36 PSU, the oxygen concentration could range from 200 to 300 µmol kg^{-1}, which would lead to high foraminiferal I / Ca. Oxygen concentrations vary considerably with latitude, with the majority of low oxygen concentration being found between 30° N and 30° S. However, oxygen reduction appears to be a more important factor than solubility (and therefore temperature) to explain the latitudinal I / Ca variability.

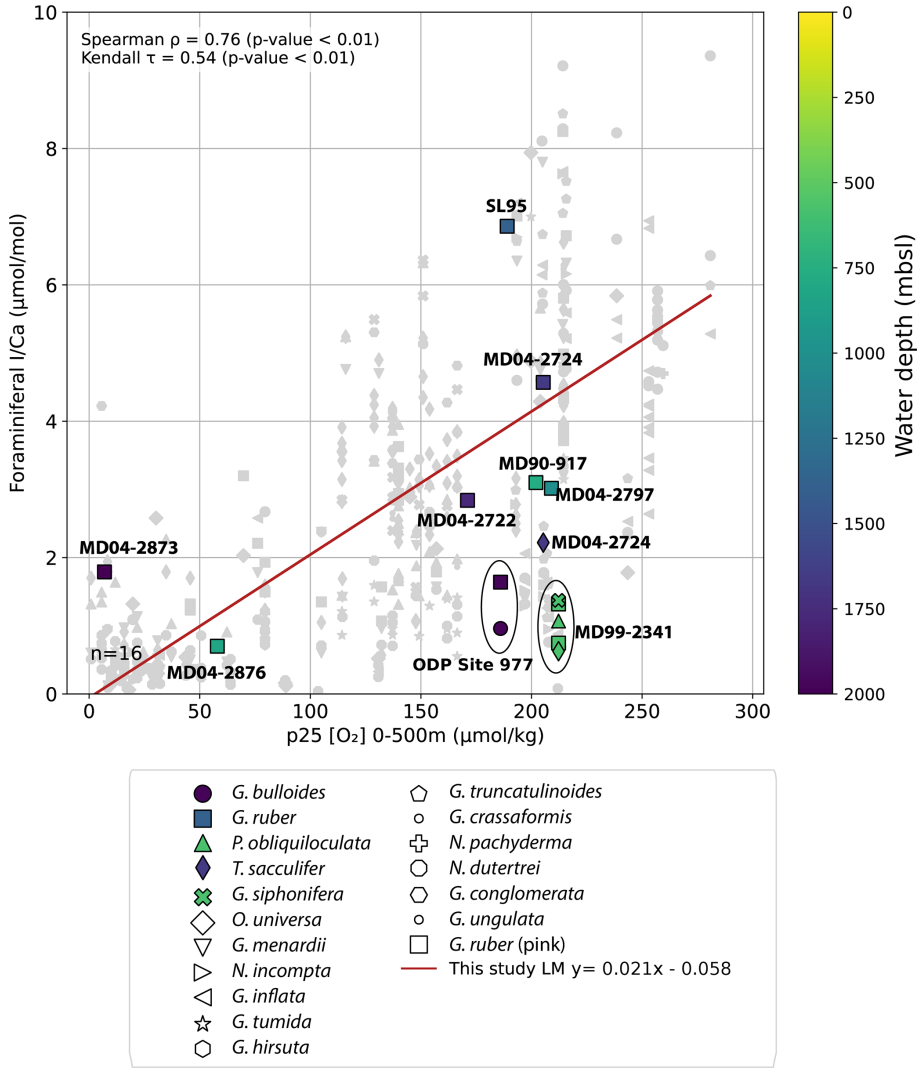

Figure 4. Core top foraminiferal I / Ca (µmol mol^{-1}) as a function of p25 [O_2] concentration (µmol kg^{-1}) for samples more recent than 8 ka BP (8000 years Before Present). New measures ($n = 15$) from this study are coloured as water depth (m b.s.l.) and identified with colour code. Previously published values are represented in grey. All foraminiferal species are differentiated by symbols. Red linear regression was obtained using all data < 2 ka BP.

Depth in core and sediment age are examined to evaluate a potential early diagenesis effect. Most of the core top selected for this study are sampled close to the water-sediment interface and in various environments. Those two variables do show statistically significant correlation with foraminiferal I / Ca on global scale. However, the number of data used for age is low ($n = 61$) and the correlation coefficients for depth in core is low. Water depth at sampling site is not correlated to foraminiferal I / Ca, as it was shown with Fig. 4.

3.5 Multi-species foraminiferal I / Ca and calcification depths on global scale

Symbiont presence in foraminifera could also alter the incorporation of specific elements like anions because of so-called "vital effects" (Hönisch et al., 2003). We have classified the symbiosis behaviour of the species and represent their I / Ca as a function of p25 [O_2] (Fig. S3), we note the absence of specific patterns. No group is enriched or depleted in iodine compared to the others. The slopes for linear regression are very close (0.016 or 0.017). Symbiont barren species are found in all defined domains, but the low I / Ca plankton tow with p25 [O_2] concentration > 250 µmol kg^{-1} are exclusively symbiont barren species.

Table 2. Results of statistical correlation test for environmental variables and planktonic foraminiferal I / Ca for samples more recent than 2 ka BP (core-tops only). Tested parameters are listed from highest to lowest absolute Spearman's ρ.

Variable	n	Spearman ρ	Spearman p-value	Kendall τ	Kendall p-value	Data source
p25_Oxygen*	406	0.78	< 0.01	0.58	< 0.01	WOD23
min_Oxygen*	406	0.78	< 0.01	0.56	< 0.01	WOD23
all_depth_mean_Oxygen*	404	0.77	< 0.01	0.58	< 0.01	WOD23
mean_Oxygen*	406	0.76	< 0.01	0.57	< 0.01	WOD23
oxycline_oxygen_mean*	224	0.72	< 0.01	0.53	< 0.01	WOD23
mean_deep_Oxygen*	427	0.65	< 0.01	0.45	< 0.01	WOD23
max_500m_depth MLD*	431	0.64	< 0.01	0.46	< 0.01	CMEMS GLORYS12V1
mean_500m_depth MLD*	431	0.63	< 0.01	0.44	< 0.01	CMEMS GLORYS12V1
mean_Phosphate*	266	−0.62	< 0.01	−0.46	< 0.01	WOD23
mean_Alkalinity*	71	−0.56	< 0.01	−0.40	< 0.01	WOD23
NPP_VGPM*	426	−0.44	< 0.01	−0.30	< 0.01	Orca Ocean Productivity
min_pH*	109	0.42	< 0.01	0.26	< 0.01	WOD23
Age (ka BP)*	61	−0.39	< 0.01	−0.29	< 0.01	See database
mean_pH*	109	0.33	< 0.01	0.31	< 0.01	WOD23
mean_Nitrate*	236	−0.28	< 0.01	−0.18	< 0.01	WOD23
mean_500m_depth velocity*	431	0.27	< 0.01	0.18	< 0.01	See database
distance to coast (km)*	431	0.27	< 0.01	0.18	< 0.01	Calculated
mean_Salinity*	389	0.24	< 0.01	0.17	< 0.01	See database
Latitude*	431	−0.14	< 0.01	−0.10	< 0.01	See database
max_Chlorophyll_depth	170	−0.14	0.08	−0.08	0.13	WOD23
Depth in core (cm)*	408	−0.13	< 0.01	−0.09	< 0.01	See database
oxycline_depth_mean	376	−0.10	0.06	−0.05	0.17	WOD23
max_Chlorophyll	170	−0.08	0.31	−0.08	0.16	WOD23
Water depth (m)	431	0.08	0.11	0.04	0.20	WOD23
max_500m_depth velocity	431	−0.06	0.22	−0.04	0.24	CMEMS GLORYS12V1
mean_Temperature	389	0.00	0.94	0.02	0.50	WOD23
max_Oxygen	406	0.00	0.98	−0.02	0.63	WOD23

* Statistically significant correlations.

In the database, we have also classified species in three zones of calcification depths as the local concentration of iodate changes with depth and influences foraminiferal I / Ca (Hess et al., 2025). Species are classified as surface, shallow subsurface, and deep subsurface dwellers following Hess et al. (2025). Figure S4 presents the linear fit of the I / Ca ratios and p25 [O_2] for Atlantic, Pacific and Indian oceans, which are obtained by classifying foraminifera according to their calcification depth. The main result is a similar slope for the three groups in Atlantic and Pacific oceans (0.017 to 0.025). Linear regressions for the Indian ocean were not plotted as 48 points are represented and the majority are located below 60 µmol kg^{-1}. Differences in intercepts are not interpreted due to the important impact of scattering. The pattern of lower I / Ca for deep subsurface dwellers in Pacific OMZs (Hess et al., 2025) is still visible, but is now located between 100 and 180 µmol kg^{-1} due to the use of p25. The Pacific Ocean is the only one where this specificity is observed.

4 Discussion

A gain in iodine in foraminiferal test during their post-mortem settling to the seafloor was proposed to explain low plankton tow values (Winkelbauer et al., 2023). This implies an increase in I / Ca with water depth. However, water depth does not show any significant covariation with foraminiferal I / Ca (Table 2 and Fig. S5). We thus consider that the influence of iodine accumulation during the foraminifera settling would be secondary and could be hidden under a stronger oxygen control. No specific pattern for foraminiferal I / Ca as a function of oxygen can be highlighted by using foraminiferal species, calcification depth groups, or symbiont presence/absence.

In the following, we will at first discuss the possible reasons for a larger scatter observed between iodate proportion and p25 [O_2] (Fig. 3). Then, a new calibration of foraminiferal I / Ca ratios against p25 [O_2] will be proposed (Fig. 5). The influence of the scattered relationship between iodate proportion and p25 [O_2] on the calibration will be evaluated (Fig. 6). Then, we will quantify residuals that are not supported by oxygenation changes to identify parameters

affecting foraminiferal I / Ca (Table S1). A comparison between foraminiferal I / Ca and the value of synthetic calcite will provide us possible impact of vital effects (Fig. 6). Finally, we will examine the contribution of authigenic calcite to the Mediterranean samples (Fig. 7) that are characterised by low I / Ca ratios under oxic condition (Fig. 4).

4.1 Principal role of oxygen and possible reasons for a larger scatter observed between iodate proportion and p25 [O_2]

First order results suggest clear covariation of foraminiferal I / Ca with oxygen and oxygen related variables (Table 2 and Fig. S5). Oxygen variables show a positive trend with foraminiferal I / Ca. This covariation ranges from linear to exponential, and displays substantial scatter. Other parameters exhibit no consistent relationship, except oxygen-linked variables such as nutrients, NPP, and mixed-layer depth (Table 2 and Fig. S2).

Inorganic iodine speciation is theoretically controlled by redox potential, largely governed by oxygen availability (Luther, 2023). In practice, however, field observations frequently deviate from this thermodynamic framework (Fig. 3). The relationship between iodate and p25 [O_2] is strongly non-linear and exhibits important scatter. The dispersion likely reflects spatial and temporal variability in iodine redox cycling across regions and seasons, and water mass mixing. This mismatch between oxygen and iodate concentration may at least partly explain the apparent presence of iodide in waters here defined as well-oxygenated.

As iodine speciation is sensitive to short-term oxygen fluctuations and depth-specific redox structure, this statistical approach better represents the oxygen conditions than relying on the minimum value. The observed scatter likely reflects a combination of true environmental heterogeneity and the limitations of matching discrete iodine measurements with oxygen data. The iodate–oxygen relationship in Fig. 3 shows that iodate proportion does not decline uniformly with decreasing oxygen. Consequently, at low p25 [O_2], the variability in the proportion of iodate can generate substantial scatter in foraminiferal I / Ca, potentially producing a factor of ~ 5 spread (1.0–5.0 µmol mol^{-1}) near 50 µmol kg^{-1}. Therefore, uncertainty in inorganic iodine speciation, both estimation errors or natural variability, remains a major source of scatter in the I / Ca–oxygen relationship.

4.2 A new calibration of planktonic foraminiferal I / Ca using p25 [O_2]

In our calibration, we use foraminiferal I / Ca as a function of p25 [O_2] concentration in 0–500 m, a representative value for oxygen concentration at each sampling site. This calibration should be used with caution for quantitative oxygen reconstruction due to substantial residual scatter. Its purpose is rather to explore the extent to which oxygen relationships can explain the observed variance.

Figure 5 shows core top samples more recent than 2 ka BP considering possible temporal changes in dissolved oxygen concentration in the ocean. The linear fit shown in red in Fig. 5 corresponds to a Least Absolute Deviations (LAD) regression. This method was selected because it is more robust to outliers and large deviations than ordinary least squares. Its reliance on medians rather than means makes it particularly suitable when the error structure is non-Gaussian or affected by outliers.

The obtained new calibration equation is as follows:

$$\text{Planktonic foraminiferal I / Ca (µmol mol}^{-1}) = 0.021 \cdot \text{p25[O}_2\text{](µmol kg}^{-1}) - 0.058 \quad (1)$$

Equation (1) provides a slightly better fit regarding precedent calibration from Hess et al. (2025) as shown by RMSE (Fig. 5a, b). This comparison integrates the recent results published by Nilsson-Kerr et al. (2025). The main difference between the two calibrations is that the clustered point at near-zero oxygen has been expanded in our case, covering a wider range of oxygen concentrations. Also, the intercept is lower, approaching I / Ca = 0 µmol mol^{-1} in strongly oxygen depleted waters (p25 [O_2] < 10 µmol kg^{-1}). The points with low I / Ca (< 2 µmol mol^{-1}) in oxygenated water correspond to samples from the Mediterranean Sea (this study) and from Southern Benguela (Lu et al., 2020).

In order to identify secondary parameters that may influence foraminiferal I / Ca, the residuals are calculated using Eq. (1). The residuals are then plotted against multiple ocean variables (Fig. S6). Table S1 summarises the correlation coefficients and significance of the parameters tested. No clear nor visible trend can be highlighted within the global dataset including water depth, distance to coast, or oxycline depth.

4.3 A comparison of the I / Ca ratio of foraminifera with the value of synthetic calcite

We further compare the new calibration with the relationship proposed for synthetic calcite (Zhou et al., 2014). The experience of synthetic calcite precipitation in iodate-rich medium indicated a linear relationship between calcite I / Ca and iodate concentration (Lu et al., 2010; Zhou et al., 2014). For the comparison, the iodate concentration in the medium is converted to oxygen concentration using the relationship between iodate proportion and p25 [O_2] concentration (Fig. 3a). Total inorganic iodine concentration is considered to be 471 nM (Fig. 3c) and calcite is assumed to be precipitated at 19 °C. The modelled abiotic I / Ca is based on inorganic iodine speciation (Fig. 3a) giving the proportion of iodate at each p25 [O_2] value. Using the mean total inorganic iodine concentration (Fig. 3c) we obtain a mean iodate concentration at different p25 [O_2]. The next step of the model is the incorporation of the iodine in the calcite lattice. Zhou et

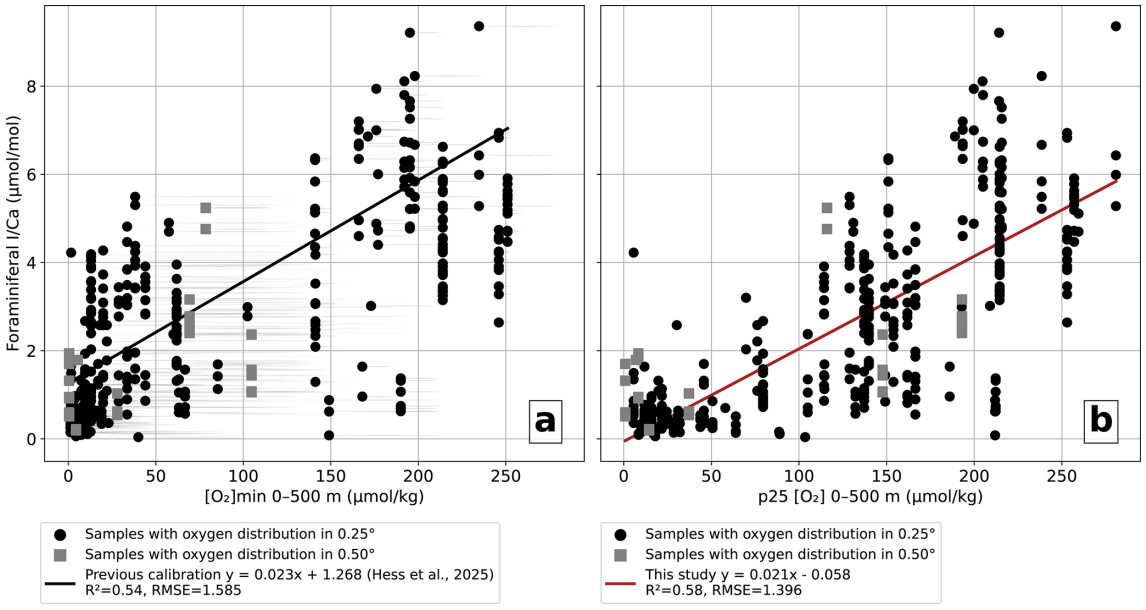

Figure 5. Foraminiferal I / Ca < 2 ka BP as a function of minimum **(a)** and p25 **(b)** [O_2] in 0–500 m. The same dataset is used for the two figures. Only the x-axis definition is different. Black line is the linear model calibration curve from (Hess et al., 2025). The red line is the linear model proposed in this study. Samples with oxygen distribution from 0.25° area are represented as black circles, and from 0.5° as grey squares. Horizontal lines in (a) illustrate the effect of x-axis change on dataset, highlighting that many low [O_2]min sites are shifted to higher representative oxygen depletion p25[O_2]. This is especially true for [O_2]min $< 50\,\mu mol\,kg^{-1}$ and I / Ca $> 2\,\mu mol\,mol^{-1}$. No specific pattern emerges within the wider area.

al. (2014) have synthetised calcite at different iodate concentrations at 6, 19 and 33 °C. They showed linear incorporation of iodine in calcite with iodate concentration. We choose to use 19 °C and examine the influence of temperature considering the case of 33 and 6 °C. The aim of this model is to investigate the possible I / Ca values considering only abiotic incorporation in calcite to evaluate possible vital effects.

In Fig. 6, the synthetic calcite I / Ca relationship is shown in blue, with the 95 % prediction interval (blue shaded area). The 95 % prediction interval is large, implying a large potential impact on our calibration. This indicates that iodate concentration relative to oxygen plays a key role in generating the observed dispersion in foraminiferal I / Ca. The modelled abiotic I / Ca only accounts for inorganic iodine speciation and temperature between 6 and 33 °C, not for total inorganic iodine concentration. The abiotic incorporation of iodine is of the same order of magnitude as that found in foraminifera. Iodine incorporation into carbonates likely reflects predominantly abiotic processes. However, some foraminiferal I / Ca ratio falls out of the prediction interval, both with p25 or minimum oxygen. Below $200\,\mu mol\,kg^{-1}$ p25[O_2], most I / Ca values are below the values that can be explained by abiotic calcite precipitation, until severe oxygen depletion ($< 20\,\mu mol\,kg^{-1}$) where foraminifera I / Ca return to the abiotic level. The highest foraminiferal I / Ca values ($> 6\,\mu mol\,mol^{-1}$) are in the highly oxygenated areas ($> 180\,\mu mol\,kg^{-1}$) and are above the abiotic interval (Fig. 6a). Those observations suggest the presence of unknown parameters that are specific for foraminiferal calcite (e.g. microenvironment, changes to growth rate . . .). Zhou et al. (2014) showed the temperature dependency of partition coefficient (K_d) of iodine for abiotic calcite. But no systemic behaviour could be highlighted explaining higher or lower foraminiferal I / Ca anomalies with temperature differences (Fig. 6). The use of min[O_2] leads to similar conclusions with I / Ca values below the 95 % prediction interval of abiotic iodine incorporation (Fig. S7b). The main difference is the high density of data points next to origin, resulting from the definition of the x-axis.

High I / Ca ratios may reflect the presence of other calcium carbonate phases, as aragonite incorporates more iodine than calcite (Hardisty et al., 2017; Lu et al., 2022). The highest I / Ca value in the Mediterranean Sea is found in the Gulf of Sirte in core SL95. This area shows high aragonite concentrations due to the presence of *Halimeda* (Reitz and De Lange, 2006). Remaining aragonite needles after cleaning may result in higher I / Ca. We investigate the influence of the presence of aragonite with binary mixing between aragonite and foraminifera. We consider an I / Ca of $10\,\mu mol\,mol^{-1}$ in aragonite, similar as the ratio measured in scleractinian corals (Sun et al. 2023). For foraminiferal I / Ca, we consider an expected value of $4\,\mu mol\,mol^{-1}$ using the new calibration and an oxygen concentration at SL95 site (Fig. 6). Aragonite contribution should be around 40 % to account for

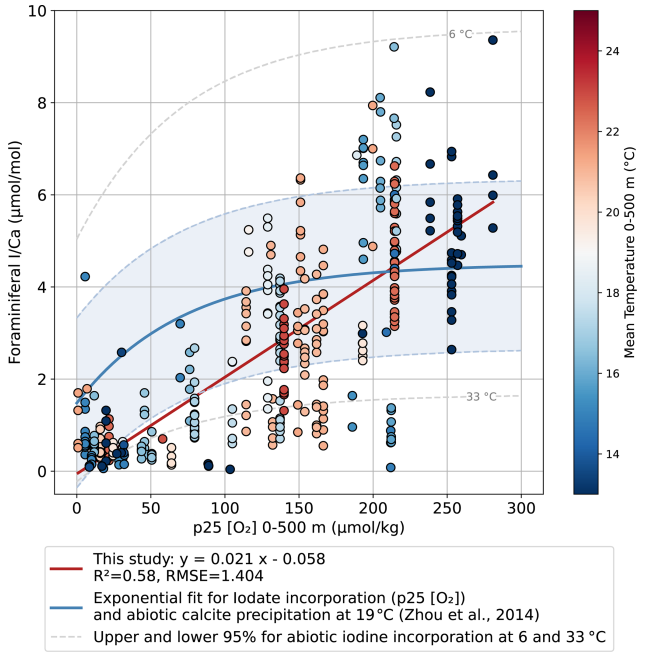

Figure 6. Foraminiferal I / Ca < 2 ka BP as a function of p25 [O_2] in 0–500 m. The red line is the linear model proposed in this study. Blue curve represents the abiotic incorporation of iodine following iodate proportion in total inorganic iodine determined in Figure 3 and assuming a mean concentration of total inorganic iodine of 471 nM (Fig. 3c). The abiotic incorporation was determined following Zhou et al. (2014). Blue area corresponds to 95 % prediction interval also determined in Fig. 4 for a temperature of 19 °C. 61 % of the data fall in this prediction interval. Temperature from 6 to 33 °C are considered for the maximum and minimum 95 % prediction interval (grey dashed lines).

an I / Ca between 6 and 7 µmol mol^{-1}, a similar range of the observed I / Ca of 6.9 µmol mol^{-1} at site SL95. Sr / Ca of these mixtures would be 4.8 and 3.9 mmol mol^{-1}, respectively, considering a Sr / Ca of 10 mmol mol^{-1} for aragonite and 1.3 mmol mol^{-1} for foraminifera (Hathorne et al., 2013; Lea et al., 1999). As the Sr / Ca from SL95 core-top is 1.345 mmol mol^{-1}, the mixture does not correspond to the observed value. The contribution of aragonite alone cannot explain the measured I / Ca value.

To summarise, inorganic iodine speciation has a non-linear relationship with dissolved oxygen concentration although the observed pattern for foraminiferal I / Ca does not follow the exponential trend that is expected from the relationship between iodate proportion and p25 [O_2] (Fig. 6a). Low I / Ca values found in oxygenated areas might be caused by reduced iodine incorporation, related to unknown mechanisms/conditions. Since no mechanism has yet been identified to justify a specific fitting curve for I / Ca ratio, we consider that the linear regression is a reasonable approximation. The dispersion of I / Ca values might be caused by the relationship between iodine speciation and oxygen concentration that could account for ~ 70 % of the variance compatible with the model's 95 % prediction interval (assuming constant total inorganic iodine), and up to ~ 87 % by considering $\pm 1\sigma$ uncertainty in total inorganic iodine from Fig. 4b (Fig. S8a). This dispersion likely represents the second key explanation for I / Ca values in foraminifera. Given its systematic offset from the predicted values, low I / Ca in highly oxygenated water seems to be related to an incorporation mechanism which remains unknown. No geographical trend could be highlighted for I / Ca below the 95 % prediction interval using p25 (Fig. 6) or using the minimum (Fig. 8c and d) oxygen. Temperature may also affect the I / Ca (Zhou et al., 2014). However, Gulf of Cadix I / Ca are 0.75 and 0.69 µmol mol^{-1} for *G. ruber* and *G. bulloides*, respectively. The two species are known to calcify in different seasons, where minimum temperature measured is 11.26 °C, and maximum is 24.21°C in 0–500 m. At ODP Site 977, I / Ca from *G. bulloides* is 0.69 and from *G. ruber* is 1.64 µmol mol^{-1}. This is the inverse of what the temperature effect predicts, with here the warm season calcifier having a higher I / Ca. So, the temperature effect may not explain all the observed values below 95 % prediction interval of abiotic I / Ca. This offset could potentially be related to the vital effects of discriminating iodine incorporation, or to local iodine speciation itself. Alternatively, it could be due to the mixing of iodate-depleted water in oxygenated water masses. However, iodate/oxygen-depleted water cannot be identified close to the Gulf of Cadix (Fig. S8b and d).

4.4 Authigenic contribution via diagenetic calcite precipitation

Depth in core and age were not significantly correlated with foraminiferal I / Ca based on first-order statistical tests (Table 2). However, these parameters do not fully capture the potential influence of diagenesis or diagenetic calcite precipitation, which may be particularly important within the sediments from within OMZs and the Mediterranean Sea which are characterised by high alkalinity pore/bottom waters. This section therefore examines whether early diagenetic carbonate precipitation could contribute to the observed variability in I / Ca.

Because authigenic carbonates typically have very low I / Ca (Lu et al., 2010), the lower I / Ca value of MD04-2876 (Arabian Sea, OMZ core) relative to MD04-2873 (below the OMZ) could partly reflect the presence of authigenic carbonates formed under reducing conditions. In the marine sediments of the OMZ, the increase in alkalinity of the pore water due to anaerobic respiration leads to the precipitation of authigenic carbonates (Suess, 1979; Meister et al., 2022). In the Mediterranean Sea, high water-column alkalinity driven by excess evaporation (Schneider et al., 2007) promotes authigenic carbonate precipitation, as shown by high Mg / Ca ratios in foraminifera (Boussetta et al., 2011).

Figure 7 presents p25 [O_2] alongside the expected foraminiferal I / Ca predicted from Eq. (1) with a red line.

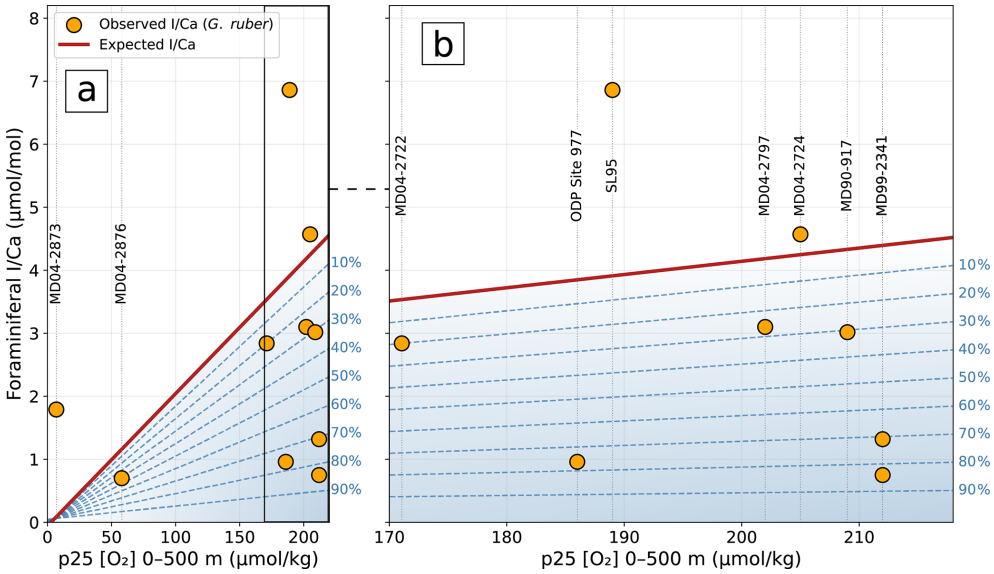

Figure 7. Foraminiferal I / Ca from the Mediterranean and Arabian Sea as a function of p25 [O_2] 0–500 m in whole p25 [O_2] range **(a)** and for p25 [O_2] >180 µmol kg^{-1} **(b)**. Expected foraminiferal I / Ca from LAD from Fig. 5 is represented as red line. Blue dotted lines indicates deviation from expected value by increasing authigenic carbonate contribution from 10 % to 90 %. Authigenic carbonate I / Ca was fixed at 0.06 µmol mol^{-1} following Lu et al. (2010).

Sensitivity tests were performed using a binary mixing model between the expected foraminiferal I / Ca and authigenic carbonates assuming an I / Ca of 0.06 µmol mol^{-1} for authigenic carbonate (Lu et al., 2010). For the Arabian Sea OMZ core, measured I / Ca values fall below the expected ratio and could correspond to a 30 %–40 % mass contribution of low I / Ca diagenetic carbonate. In contrast, MD04-2873 (below the OMZ) displays higher I / Ca than expected, likely due to poorly constrained oxygen variability resulting from the limited number of available oxygen profiles (Sect. 3.1).

In the Mediterranean Sea, the two eastern basin cores (SL95 and MD04-2724) show I / Ca values above expectation, while others fall below. Cores MD04-2722, MD04-2797 and MD90-917 are slightly depleted in I / Ca relative to the value estimated from Eq. (1) and could reflect a 20 %–30 % contribution of authigenic carbonates. However, the samples from the western basin (ODP Site 977) and from the Gulf of Cadiz (MD99-2341) would require an implausibly high 60 %–90 % contribution of authigenic calcite to explain their (much-)lower-than-expected I / Ca. Such a contribution is unrealistic, as authigenic calcite precipitation is far less common in the western basin, and extensive overgrowths would have been excluded (Crudeli et al., 2004).

Overall, diagenetic calcite precipitation cannot fully explain the lower I / Ca deviations. Low I / Ca values occur in regions where early diagenetic calcite formation is low, while no mechanism has been identified to account for I / Ca values higher than expected, nor for the scatter observed among species dwelling at the same depth within the same core top samples, except for as yet undefined vital effects.

We conclude that foraminiferal I / Ca primarily reflects local oxygen variability through its control on iodine speciation. The Mediterranean Sea samples exhibit a similar behaviour and degree of scatter between I / Ca and p25 [O_2] as those from other ocean basins, indicating that the proxy remains applicable in this semi-enclosed environment. While foraminiferal I / Ca provides a semi-quantitative estimation of local oxygenation conditions, the core-top values observed in the western Mediterranean Sea is lower than the values expected from the calibration. The use of the proxy must focus on relative variability combined with another independent approach. The relationship between foraminiferal I / Ca and oxygen concentration may be site-specific, because it could be influenced by local environmental characteristics or processes that are not yet fully understood. This limitation is particularly relevant for coastal sites, including those within the Mediterranean Sea, where additional factors may modulate iodine speciation or iodine incorporation.

4.5 Other possible factors

Oceanographic variables investigated other than oxygen did not show strong relationship with foraminiferal I / Ca (Table 2). Other parameters may also influence iodine speciation but were not highlighted through the statistical analysis conducted on foraminiferal I / Ca in this study. Previous works have shown that iodine speciation varies with distance to the coast, with iodate depletion toward productive coastal water (Wong and Zhang, 1992). The effect of distance to coast is absent on global scale, but it could be important at regional scale, such as in the Mediterranean Sea.

This depletion is thought to be driven by enhanced biological iodine uptake through primary productivity. Although the Mediterranean Sea is highly oligotrophic, coastal and shelf regions can sustain episodes of high primary productivity (Packard et al., 1988; Powley et al., 2017), which could potentially influence iodate concentration. Only limited inorganic iodine vertical profiles (iodate and iodide) exists in the Mediterranean Sea (Fig. 1b), with one time series in the north western basin (Tian and Nicolas, 1995). The study showed limited variability across the year with iodate concentrations of 410–480 nM, but iodine speciation was measured in different oceanographic settings as the investigated locations in this study. Even though different inorganic iodine behaviours cannot be ruled out, the variability of iodate concentration observed in the north western Mediterranean Sea, about 10 %, does not explain the scattering in I / Ca observed.

Part of the variability may also not be fully constrained with the statistical analysis conducted (Tables 2 and S1, Figs. S2 and S5). In fact, we conducted the analysis on the global dataset, with every site being a unique context and oceanographic settings. If we highlighted the first and most important role of oxygen as an I / Ca control, secondary parameters may not be fully captured. Inorganic iodine speciation remains poorly understood. Also, the influence of growth rate (calcification kinetics) could not be ruled out, and was never tested for I / Ca ratio (e.g. Allen et al., 2016). This has not been demonstrated but competition with other anions remains plausible as coupled substitution is required for the incorporation of IO_3^- into $CaCO_3$ (Ram and Erez, 2023).

Cheng et al. (2026) have investigated inorganic iodine speciation in the Baltic Sea, another semi-enclosed basin. They have shown decoupled iodine and oxygen concentrations in surface water, with a low iodate concentration in oxygenated water. This observation would result in low foraminiferal I / Ca in apparently oxygenated water. The low I / Ca ratio can be explained by the iodate uptake by primary producers, and an efficient iodine removal with organic matter under hypoxic conditions. In contrast, the Mediterranean Sea is an oligotrophic basin where iodate uptake by primary producers is expected to be small. Although episodic oxygen depletion driven by interannual variability (Coppola et al., 2018) could potentially lead to iodate reduction, available data indicate that the concentration of dissolved iodate is high, ranging from 410 to 480 nM in the western basin, and from 380 to 550 nM in the eastern basin (Tian and Nicolas, 1995; Ullman et al., 1990), far from the 100 nM found in the Baltic Sea (Cheng et al., 2026).

In light of these observations, we emphasise the use of foraminiferal I / Ca as a semi-quantitative proxy for changes in ocean oxygenation. The proxy primarily responds to oxygen and oxygen-related parameters (Table 2, Fig. S5, Supplement Table S1 and Fig. S6). The p25[O_2] gave the best fit with less data dispersion (Fig. S1). The dispersion of the relationship between inorganic iodine speciation and p25[O_2] partly accounts for mixing and differences in inorganic iodine redox kinetics. For these reasons together with potential non-investigated parameters, foraminiferal I / Ca alone cannot be interpreted as a quantitative proxy. Combining it with other proxies and/or a modelling approach is highly recommended. However, it may still be highly informative about changes in oxygen at a specific site. The calibration is useful, not for absolute oxygen reconstruction, but to understand site-specific I / Ca variation relative to the observed oxygen range and identify sites where high I / Ca in oxygenated waters provides the best sensitivity to past oxygenation change. However, most studies focused oxygen depleted areas, leading to less representation of oxygenated and high latitudes sites in the dataset. Wang et al. (2026) proposed oxygen thresholds to interpret foraminiferal I / Ca. However, the current global data set would be biased towards oxygen–depleted areas. Our Mediterranean core-tops data show a wide I / Ca range in oxygenated waters, which cannot be explained by authigenic calcite precipitation or aragonitic carbonate presence, suggesting additional scatter introduced in oxygenated settings (e.g., vital effects, water mass mixing, local inorganic iodine speciation). Further core-top data spanning the whole oxygenation range is needed to validate the threshold behaviour and determine the reason for low foraminiferal I / Ca in oxygenated water.

For future work, foraminifera culture with isolation of single parameters/monitoring of multiple parameters could help better constrain the proxy behaviour, alongside field studies. In particular, plankton tow observations showing systematically low foraminiferal I / Ca values suggest that limited incorporation at the surface may happen, leaving open the question of when and where iodine is incorporated. Inorganic iodine speciation is still poorly constrained and further research is needed to understand its dynamics and incorporation in calcite lattice. Iodine incorporation sites and mechanisms, are hardly needed to distinguish the origin of the signal and better understand the observed trends.

5 Conclusions

In this study, we investigate planktonic foraminiferal I / Ca as a proxy for subsurface oxygen changes by integrating multiple environmental parameters. We first proposed a new definition of a representative oxygen depletion value in subsurface waters, accounting for local oxygen variability. Local oxygen distributions were unimodal or multimodal, reflecting both seasonal and depth-related oxygen variation. Planktonic foraminiferal I / Ca from core top samples showed a positive correlation with this representative minimum oxygen value, p25 [O_2], supporting the dominant control of oxygen on iodine presence and reinforcing the utility of the proxy to reconstruct past oxygenation changes.

Despite this relationship, substantial amount of data dispersion remains. We explored several potential sources of

scatter and found that the largest contribution likely arises from variability in inorganic iodine speciation. The global relationship between iodate and p25 [O_2] alone could account for more than 85 % of the observed scatter.

No first-order relationship was found between water depth and foraminiferal I / Ca. This observation implies that iodine gain during particle sinking (Winkelbauer et al., 2023) could not be confirmed.

We propose a new calibration for subsurface oxygen depletion reconstruction based on planktonic foraminiferal I / Ca. By using p25 [O_2] values, we reduce the dispersion observed in previous calibrations. To maintain simplicity for paleo-applications, core top data younger than 2 ka BP were included regardless of species. Remaining dispersion may result from vital (integration of iodate into the foraminifera shell) or species-specific effects (difference in iodate integration between species), or other uninvestigated parameters, such as inorganic iodine speciation modulated by water mass mixing, NPP, or differences in oxidoreduction kinetics.

Finally, diagenetic calcite contribution was considered as a potential contributor to the low foraminiferal I / Ca values, given that diagenetic calcite formed in high alkalinity environment could dilute the signal. However, such an effect would require more than 60 % of diagenetic calcite to explain western Mediterranean Sea values, which is implausible.

We therefore support the use of planktonic foraminiferal I / Ca as a semi-quantitative proxy for oxygenation state, consistent with Hess et al. (2025). This proxy can also be applied to semi-enclosed basins to reconstruct relative variability when complemented with another independent approach. However, foraminiferal I / Ca cannot be used as a quantitative proxy for oxygen reconstruction. The tool must be used alongside another approach to support past environmental change. These recommendations are still prone to further evolution as we better constrain the proxy and the inorganic iodine cycle in the ocean.

Data availability. Data supporting this paper is available in the following repository: https://doi.org/10.5281/zenodo.18390413 (Guarinos et al., 2026a).

Supplement. The supplement related to this article is available online at https://doi.org/10.5194/bg-23-5477-2026-supplement.

Author contributions. KT and VG designed the study; KT, MG and VG performed the laboratory procedures; VG have conducted the statistical analysis. VG wrote and edited the manuscript with contributions from all authors.

Competing interests. The contact author has declared that none of the authors has any competing interests.

Disclaimer. Publisher's note: Copernicus Publications remains neutral with regard to jurisdictional claims made in the text, published maps, institutional affiliations, or any other geographical representation in this paper. The authors bear the ultimate responsibility for providing appropriate place names. Views expressed in the text are those of the authors and do not necessarily reflect the views of the publisher.

Acknowledgements. This work is supported by the French national project ANR MedSens (ANR-19-CE01-0019) granted to KT. Radiocarbon dating was performed at the LMC14 laboratory as a part of the French ARTEMIS program. Sample preparation and analytical measurements were supported by the LPM platform (Sandrine Conrod), the LGO2i platform, and the ENVITOP platform. We also thanks Rosie Chance and Helge A. Winkelbauer for providing global iodine speciation dataset, and Rosalind E.M. Rickaby for the inspiring discussions on the topic. We thank Dalton Hardisty and the anonymous referee for their comments which greatly helped improve the manuscript. We also thank Ny Riavo G. Voarintsoa (Associate Editor, Biogeosciences) for editorial handling.

Financial support. This work is supported by the French national project ANR MedSens (ANR-19-CE01-0019) and GEOCCO project (CLIMAGO/LEFE) granted to KT.

Review statement. This paper was edited by Ny Riavo G. Voarintsoa and reviewed by Dalton Hardisty and one anonymous referee.

References

Allen, K. A., Hönisch, B., Eggins, S. M., Haynes, L. L., Rosenthal, Y., and Yu, J.: Trace element proxies for surface ocean conditions: A synthesis of culture calibrations with planktic foraminifera, Geochim. Cosmochim. Ac., 193, 197–221, https://doi.org/10.1016/j.gca.2016.08.015, 2016.

Bard, E., Ménot, G., Rostek, F., Licari, L., Böning, P., Edwards, R. L., Cheng, H., Wang, Y., and Heaton, T. J.: Radiocarbon Calibration/Comparison Records Based on Marine Sediments from the Pakistan and Iberian Margins, Radiocarbon, 55, 1999–2019, https://doi.org/10.2458/azu_js_rc.55.17114, 2013.

Barker, S., Greaves, M., and Elderfield, H.: A study of cleaning procedures used for foraminiferal Mg/Ca paleothermometry, Geochem. Geophy. Geosy., 4, https://doi.org/10.1029/2003GC000559, 2003.

Behrenfeld, M. J. and Falkowski, P. G.: Photosynthetic rates derived from satellite-based chlorophyll concentration, Limnol. Oceanogr., 42, 1–20, https://doi.org/10.4319/lo.1997.42.1.0001, 1997.

Bopp, L., Resplandy, L., Orr, J. C., Doney, S. C., Dunne, J. P., Gehlen, M., Halloran, P., Heinze, C., Ilyina, T., Séférian, R., Tjiputra, J., and Vichi, M.: Multiple stressors of ocean ecosystems in the 21st century: projections with CMIP5 models, Biogeosciences, 10, 6225–6245, https://doi.org/10.5194/bg-10-6225-2013, 2013.

Boussetta, S., Bassinot, F., Sabbatini, A., Caillon, N., Nouet, J., Kallel, N., Rebaubier, H., Klinkhammer, G., and Labeyrie, L.: Diagenetic Mg-rich calcite in Mediterranean sediments: Quantification and impact on foraminiferal Mg/Ca thermometry, Mar. Geol., 280, 195–204, https://doi.org/10.1016/j.margeo.2010.12.011, 2011.

Chai, J. Y. and Muramatsu, Y.: Determination of Bromine and Iodine in Twenty-three Geochemical Reference Materials by ICP-MS, Geostand. Geoanal. Res., 31, 143–150, https://doi.org/10.1111/j.1751-908X.2007.00856.x, 2007.

Chance, R., Weston, K., Baker, A. R., Hughes, C., Malin, G., Carpenter, L., Meredith, M. P., Clarke, A., Jickells, T. D., Mann, P., and Rossetti, H.: Seasonal and interannual variation of dissolved iodine speciation at a coastal Antarctic site, Mar. Chem., 118, 171–181, https://doi.org/10.1016/j.marchem.2009.11.009, 2010.

Chance, R., Baker, A. R., Carpenter, L., and Jickells, T. D.: The distribution of iodide at the sea surface, Env. Sci. Process. Impacts, 16, 1841–1859, https://doi.org/10.1039/C4EM00139G, 2014.

Chance, R., Tinel, L., Sarkar, A., Sinha, A. K., Mahajan, A. S., Chacko, R., Sabu, P., Roy, R., Jickells, T. D., Stevens, D. P., Wadley, M., and Carpenter, L. J.: Surface Inorganic Iodine Speciation in the Indian and Southern Oceans From 12° N to 70° S, Front. Mar. Sci., 7, 621, https://doi.org/10.3389/fmars.2020.00621, 2020.

Chance, R. J., Tinel, L., Sherwen, T., Baker, A. R., Bell, T., Brindle, J., Campos, M. L. A. M., Croot, P., Ducklow, H., Peng, H., Hopkins, F., Hoogakker, B., Hughes, C., Jickells, T. D., Loades, D., Macaya, D. A. R., Mahajan, A. S., Malin, G., Phillips, D., Roberts, I., Roy, R., Sarkar, A., Sinha, A. K., Song, X., Winkelbauer, H., Wuttig, K., Yang, M., Peng, Z., and Carpenter, L. J.: Global sea-surface iodide observations, 1967–2018, Sci. Data, 6, 286, https://doi.org/10.1038/s41597-019-0288-y, 2019.

Cheng, K., Ridgwell, A., and Hardisty, D. S.: Characterizing the marine iodine cycle and its relationship to ocean deoxygenation in an Earth system model, Biogeosciences, 21, 4927–4949, https://doi.org/10.5194/bg-21-4927-2024, 2024.

Cheng, K., Hansel, C. M., Carley, I., Voss, M., TerAvest, M. A., Schrenk, M. O., and Hardisty, D. S.: Observational and experimental constraints on iodine cycling in low oxygen waters, Geochim. Cosmochim. Ac., 427, 35–50, https://doi.org/10.1016/j.gca.2026.06.020, 2026.

Coppola, L., Legendre, L., Lefevre, D., Prieur, L., Taillandier, V., and Diamond Riquier, E.: Seasonal and inter-annual variations of dissolved oxygen in the northwestern Mediterranean Sea (DYFAMED site), Prog. Oceanogr., 162, 187–201, https://doi.org/10.1016/j.pocean.2018.03.001, 2018.

Cornuault, M., Tachikawa, K., Vidal, L., Guihou, A., Siani, G., Deschamps, P., Bassinot, F., and Revel, M.: Circulation Changes in the Eastern Mediterranean Sea Over the Past 23,000 Years Inferred From Authigenic Nd Isotopic Ratios, Paleoceanogr. Paleoclimatology, 33, 264–280, https://doi.org/10.1002/2017PA003227, 2018.

Crudeli, D., Young, J. R., Erba, E., De Lange, G. J., Henriksen, K., Kinkel, H., Slomp, C. P., and Ziveri, P.: Abnormal carbonate diagenesis in Holocene–late Pleistocene sapropel-associated sediments from the Eastern Mediterranean; evidence from Emiliania huxleyi coccolith morphology, Mar. Micropaleontol., 52, 217–240, https://doi.org/10.1016/j.marmicro.2004.04.010, 2004.

Elderfield, H. and Truesdale, V. W.: On the biophilic nature of iodine in seawater, Earth Planet. Sc. Lett., 50, 105–114, https://doi.org/10.1016/0012-821X(80)90122-3, 1980.

Evans, N., Boles, E., Kwiecinski, J. V., Mullen, S., Wolf, M., Devol, A. H., Moriyasu, R., Nam, S., Babbin, A. R., and Moffett, J. W.: The role of water masses in shaping the distribution of redox active compounds in the Eastern Tropical North Pacific oxygen deficient zone and influencing low oxygen concentrations in the eastern Pacific Ocean, Limnol. Oceanogr., 65, 1688–1705, https://doi.org/10.1002/lno.11412, 2020.

Eynaud, F., De Abreu, L., Voelker, A., Schönfeld, J., Salgueiro, E., Turon, J., Penaud, A., Toucanne, S., Naughton, F., Sánchez Goñi, M. F., Malaizé, B., and Cacho, I.: Position of the Polar Front along the western Iberian margin during key cold episodes of the last 45 ka, Geochem. Geophy. Geosy., 10, 2009GC002398, https://doi.org/10.1029/2009GC002398, 2009.

Farrenkopf, A. M. and Luther III, G. W.: Iodine chemistry reflects productivity and denitrification in the Arabian Sea: evidence for flux of dissolved species from sediments of western India into the OMZ, Deep-Sea Res. Pt. II, 49, 2303–2318, https://doi.org/10.1016/S0967-0645(02)00038-3, 2002.

Feng, X. and Redfern, S. A. T.: Iodate in calcite, aragonite and vaterite $CaCO_3$: Insights from first-principles calculations and implications for the I/Ca geochemical proxy, Geochim. Cosmochim. Ac., 236, 351–360, https://doi.org/10.1016/j.gca.2018.02.017, 2018.

Frölicher, T. L., Rodgers, K. B., Stock, C. A., and Cheung, W. W. L.: Sources of uncertainties in 21st century projections of potential ocean ecosystem stressors, Global Biogeochem. Cy., 30, 1224–1243, https://doi.org/10.1002/2015GB005338, 2016.

Guarinos, V., Tachikawa, K., Garcia Molina, M., Siani, G., Revel, M., Schulz, H., Sierro, F., and Chalk, T.: Dataset: Guarinos et al., 2026 article "Planktonic foraminifera Iodine / Calcium ratio: is it a proxy for dissolved oxygen in the ocean?", Zenodo [data set], https://doi.org/10.5281/zenodo.18390413, 2026a.

Guarinos V., Tachikawa K., Ayache M., Dutay J.-C., Pérez-Asensio J. N., Chalk T. B., Conrod S., Siani G., Schulz H., Revel M., Sierro F. J., and Vidal L.: Mediterranean Sea oxygenation state in early Holocene: a proxy and model approach, in preparation, 2026b.

Hardisty, D. S., Lu, Z., Bekker, A., Diamond, C. W., Gill, B. C., Jiang, G., Kah, L. C., Knoll, A. H., Loyd, S. J., Osburn, M. R., Planavsky, N. J., Wang, C., Zhou, X., and Lyons, T. W.: Perspectives on Proterozoic surface ocean redox from iodine contents in ancient and recent carbonate, Earth Planet. Sc. Lett., 463, 159–170, https://doi.org/10.1016/j.epsl.2017.01.032, 2017.

Hardisty, D. S., Horner, T. J., Evans, N., Moriyasu, R., Babbin, A. R., Wankel, S. D., Moffett, J. W., and Nielsen, S. G.: Limited iodate reduction in shipboard seawater incubations from the Eastern Tropical North Pacific oxygen deficient zone, Earth Planet. Sc. Lett., 554, 116676, https://doi.org/10.1016/j.epsl.2020.116676, 2021.

Hathorne, E. C., Gagnon, A., Felis, T., Adkins, J., Asami, R., Boer, W., Caillon, N., Case, D., Cobb, K. M., Douville, E., deMenocal, P., Eisenhauer, A., Garbe-Schönberg, D., Geibert, W., Goldstein, S., Hughen, K., Inoue, M., Kawahata, H., Kölling, M., Cornec, F. L., Linsley, B. K., McGregor, H. V., Montagna, P., Nurhati, I. S., Quinn, T. M., Raddatz, J., Rebaubier, H., Robinson, L., Sadekov, A., Sherrell, R., Sinclair, D.,

Tudhope, A. W., Wei, G., Wong, H., Wu, H. C., and You, C.: Interlaboratory study for coral Sr/Ca and other element/Ca ratio measurements, Geochem. Geophy. Geosy., 14, 3730–3750, https://doi.org/10.1002/ggge.20230, 2013.

He, R., Pohl, A., Zhang, X., Chang, C., Prow-Fleischer, A., Payne, J. L., Xiao, S., Ridgwell, A., and Lu, Z.: A reversed latitudinal ocean oxygen gradient in the Proterozoic Eon, Nat. Geosci., 19, 325–330, https://doi.org/10.1038/s41561-025-01896-w, 2026.

Hepach, H., Hughes, C., Hogg, K., Collings, S., and Chance, R.: Senescence as the main driver of iodide release from a diverse range of marine phytoplankton, Biogeosciences, 17, 2453–2471, https://doi.org/10.5194/bg-17-2453-2020, 2020.

Hess, A. V., Rosenthal, Y., Zhou, X., and Bu, K.: The I/Ca paleo-oxygenation proxy in planktonic foraminifera: A multispecies core-top calibration, Geochim. Cosmochim. Ac., S0016703725000298, https://doi.org/10.1016/j.gca.2025.01.018, 2025.

Hönisch, B., Bijma, J., Russell, A. D., Spero, H. J., Palmer, M. R., Zeebe, R. E., and Eisenhauer, A.: The influence of symbiont photosynthesis on the boron isotopic composition of foraminifera shells, Mar. Micropaleontol., 49, 87–96, https://doi.org/10.1016/S0377-8398(03)00030-6, 2003.

Hoogakker, B. A. A., Davis, C., Wang, Y., Kusch, S., Nilsson-Kerr, K., Hardisty, D. S., Jacobel, A., Reyes Macaya, D., Glock, N., Ni, S., Sepúlveda, J., Ren, A., Auderset, A., Hess, A. V., Meissner, K. J., Cardich, J., Anderson, R., Barras, C., Basak, C., Bradbury, H. J., Brinkmann, I., Castillo, A., Cook, M., Costa, K., Choquel, C., Diz, P., Donnenfield, J., Elling, F. J., Erdem, Z., Filipsson, H. L., Garrido, S., Gottschalk, J., Govindankutty Menon, A., Groeneveld, J., Hallmann, C., Hendy, I., Hennekam, R., Lu, W., Lynch-Stieglitz, J., Matos, L., Martínez-García, A., Molina, G., Muñoz, P., Moretti, S., Morford, J., Nuber, S., Radionovskaya, S., Raven, M. R., Somes, C. J., Studer, A. S., Tachikawa, K., Tapia, R., Tetard, M., Vollmer, T., Wang, X., Wu, S., Zhang, Y., Zheng, X.-Y., and Zhou, Y.: Reviews and syntheses: Review of proxies for low-oxygen paleoceanographic reconstructions, Biogeosciences, 22, 863–957, https://doi.org/10.5194/bg-22-863-2025, 2025.

Jickells, T. D., Boyd, S. S., and Knap, A. H.: Iodine cycling in the Sargasso Sea and the Bermuda inshore waters, Mar. Chem., 24, 61–82, https://doi.org/10.1016/0304-4203(88)90006-0, 1988.

Jones, M. R., Chance, R., Bell, T., Jones, O., Loades, D. C., May, R., Tinel, L., Weddell, K., Widdicombe, C., and Carpenter, L. J.: Iodide, iodate & dissolved organic iodine in the temperate coastal ocean, Front. Mar. Sci., 11, 1277595, https://doi.org/10.3389/fmars.2024.1277595, 2024.

Lea, D. W., Mashiotta, T. A., and Spero, H. J.: Controls on magnesium and strontium uptake in planktonic foraminifera determined by live culturing, Geochim. Cosmochim. Ac., 63, 2369–2379, https://doi.org/10.1016/S0016-7037(99)00197-0, 1999.

Lellouche, Eric, G., Romain, B.-B., Gilles, G., Angélique, M., Marie, D., Clément, B., Mathieu, H., Olivier, L. G., Charly, R., Tony, C., Charles-Emmanuel, T., Florent, G., Giovanni, R., Mounir, B., Yann, D., and Pierre-Yves, L. T.: The Copernicus Global 1/12° Oceanic and Sea Ice GLORYS12 Reanalysis, Front. Earth Sci., 9, 698876, https://doi.org/10.3389/feart.2021.698876, 2021.

Lu, W., Dickson, A. J., Thomas, E., Rickaby, R. E. M., Chapman, P., and Lu, Z.: Refining the planktic foraminiferal I/Ca proxy: Results from the Southeast Atlantic Ocean, Geochim. Cosmochim. Ac., 287, 318–327, https://doi.org/10.1016/j.gca.2019.10.025, 2020.

Lu, W., Wang, Y., Oppo, D. W., Nielsen, S. G., and Costa, K. M.: Comparing paleo-oxygenation proxies (benthic foraminiferal surface porosity, I/Ca, authigenic uranium) on modern sediments and the glacial Arabian Sea, Geochim. Cosmochim. Ac., 331, 69–85, https://doi.org/10.1016/j.gca.2022.06.001, 2022.

Lu, Z., Jenkyns, H. C., and Rickaby, R. E. M.: Iodine to calcium ratios in marine carbonate as a paleo-redox proxy during oceanic anoxic events, Geology, 38, 1107–1110, https://doi.org/10.1130/G31145.1, 2010.

Lu, Z., Hoogakker, B. A. A., Hillenbrand, C.-D., Zhou, X., Thomas, E., Gutchess, K. M., Lu, W., Jones, L., and Rickaby, R. E. M.: Oxygen depletion recorded in upper waters of the glacial Southern Ocean, Nat. Commun., 9, https://doi.org/10.1038/ncomms11146, 2016.

Luther, G. W.: Review on the physical chemistry of iodine transformations in the oceans, Front. Mar. Sci., 10, 1085618, https://doi.org/10.3389/fmars.2023.1085618, 2023.

Martrat, B., Grimalt, J. O., Lopez-Martinez, C., Cacho, I., Sierro, F. J., Flores, J. A., Zahn, R., Canals, M., Curtis, J. H., and Hodell, D. A.: Abrupt Temperature Changes in the Western Mediterranean over the Past 250,000 Years, Science, 306, 1762–1765, https://doi.org/10.1126/science.1101706, 2004.

Meister, P., Herda, G., Petrishcheva, E., Gier, S., Dickens, G. R., Bauer, C., and Liu, B.: Microbial Alkalinity Production and Silicate Alteration in Methane Charged Marine Sediments: Implications for Porewater Chemistry and Diagenetic Carbonate Formation, Front. Earth Sci., 9, 756591, https://doi.org/10.3389/feart.2021.756591, 2022.

Mishonov, A. V., Boyer, T. P., Baranova, O. K., Bouchard, C. N., Cross, S. L., Garcia, H. E., Locarnini, R. A., Paver, C. R., Reagan, J. R., Wang, Z., Seidov, D., Grodsky, A. I., and Beauchamp, J. G.: World Ocean Database 2023, NOAA, https://doi.org/10.25923/z885-h264, 2024.

Moriyasu, R., Evans, N., Bolster, K. M., Hardisty, D. S., and Moffett, J. W.: The Distribution and Redox Speciation of Iodine in the Eastern Tropical North Pacific Ocean, Global Biogeochem. Cy., 34, e2019GB006302, https://doi.org/10.1029/2019GB006302, 2020.

Nilsson-Kerr, K., Hoogakker, B. A. A., Macaya, D. A. R., Winkelbauer, H. A., Hamilton, E., Chenery, S., Davis, C. V., and Leng, M. J.: Late Cenozoic intensification of deoxygenation in the Pacific Ocean, Earth Planet. Sc. Lett., 655, 119253, https://doi.org/10.1016/j.epsl.2025.119253, 2025.

Ocean Data View: https://odv.awi.de/, last access: 10 December 2025.

ORCA Science: Ocean Productivity Data Server, http://orca.science.oregonstate.edu/index.php, last access: 17 June 2025.

Oschlies, A., Duteil, O., Getzlaff, J., Koeve, W., Landolfi, A., and Schmidtko, S.: Patterns of deoxygenation: sensitivity to natural and anthropogenic drivers, Philos. Trans. R. Soc. A, 375, 20160325, https://doi.org/10.1098/rsta.2016.0325, 2017.

Oschlies, A., Brandt, P., Stramma, L., and Schmidtko, S.: Drivers and mechanisms of ocean deoxygenation, Nat. Geosci., 11, 467–473, https://doi.org/10.1038/s41561-018-0152-2, 2018.

Packard, T. T., Minas, H. J., Coste, B., Martinez, R., Bonin, M. C., Gostan, J., Garfield, P., Christensen, J., Dortch, Q., Minas, M., Copin-Montegut, G., and Copin-Montegut, C.: Formation of the

Alboran oxygen minimum zone, Deep-Sea Res. Pt. I, 35, 1111–1118, https://doi.org/10.1016/0198-0149(88)90003-9, 1988.

Pichevin, L., Bard, E., Martinez, P., and Billy, I.: Evidence of ventilation changes in the Arabian Sea during the late Quaternary: Implication for denitrification and nitrous oxide emission, Global Biogeochem. Cy., 21, 2006GB002852, https://doi.org/10.1029/2006GB002852, 2007.

Podder, J., Lin, J., Sun, W., Botis, S. M., Tse, J., Chen, N., Hu, Y., Li, D., Seaman, J., and Pan, Y.: Iodate in calcite and vaterite: Insights from synchrotron X-ray absorption spectroscopy and first-principles calculations, Geochim. Cosmochim. Ac., 198, 218–228, https://doi.org/10.1016/j.gca.2016.11.032, 2017.

Powley, H. R., Cappellen, P. V., and Krom, M. D.: Nutrient Cycling in the Mediterranean Sea: The Key to Understanding How the Unique Marine Ecosystem Functions and Responds to Anthropogenic Pressures, in: Mediterranean Identities – Environment, Society, Culture, edited by: Fuerst-Bjelis, B., InTech, https://doi.org/10.5772/intechopen.70878, 2017.

Ram, S. and Erez, J.: Anion elements incorporation into corals skeletons: Experimental approach for biomineralization and paleo-proxies, P. Natl. Acad. Sci. USA, 120, e2306627120, https://doi.org/10.1073/pnas.2306627120, 2023.

Reitz, A. and De Lange, G. J.: Abundant Sr-rich aragonite in eastern Mediterranean sapropel S1: Diagenetic vs. detrital/biogenic origin, Palaeogeogr. Palaeocl., 235, 135–148, https://doi.org/10.1016/j.palaeo.2005.10.024, 2006.

Schneider, A., Wallace, D. W. R., and Körtzinger, A.: Alkalinity of the Mediterranean Sea, Geophys. Res. Lett., 34, 2006GL028842, https://doi.org/10.1029/2006GL028842, 2007.

Siani, G., Paterne, M., and Colin, C.: Late glacial to Holocene planktic foraminifera bioevents and climatic record in the South Adriatic Sea, J. Quaternary Sci., 25, 808–821, https://doi.org/10.1002/jqs.1360, 2010.

Suess, E.: Mineral phases formed in anoxic sediments by microbial decomposition of organic matter, Geochim. Cosmochim. Ac., 43, 339–352, https://doi.org/10.1016/0016-7037(79)90199-6, 1979.

Tian, R. C. and Nicolas, E.: Iodine speciation in the northwestern Mediterranean Sea, method and vertical profile, Mar. Chem., 48, 151–156, https://doi.org/10.1016/0304-4203(94)00048-I, 1995.

Ullman, W. J., Luther, G. W., de Lange, G. J, and Woittiez, J. R. W: Iodine chemistry in deep anoxic basins and overlying waters of the Mediterranean Sea, Mar. Chem., https://doi.org/10.1016/0304-4203(90)90036-C, 1990.

Wadley, M. R., Stevens, D. P., Jickells, T. D., Hughes, C., Chance, R., Hepach, H., Tinel, L., and Carpenter, L. J.: A Global Model for Iodine Speciation in the Upper Ocean, Global Biogeochem. Cy., 34, e2019GB006467, https://doi.org/10.1029/2019GB006467, 2020.

Wang, X., Rickaby, R. E. M., and Lu, Z.: A deep dive into the planktic foraminiferal I/Ca in global core-tops, Global Planet. Change, 105412, https://doi.org/10.1016/j.gloplacha.2026.105412, 2026.

Winkelbauer, H., Cordova-Rodriguez, K., Reyes-Macaya, D., Scott, J., Glock, N., Lu, Z., Hamilton, E., Chenery, S., Holdship, P., Dormon, C., and Hoogakker, B.: Foraminifera Iodine to Calcium Ratios: Approach and Cleaning, Geochem. Geophy. Geosy., 22, https://doi.org/10.1029/2021GC009811, 2021.

Winkelbauer, H. A., Hoogakker, B. A. A., Chance, R. J., Davis, C. V., Anthony, C. J., Bischoff, J., Carpenter, L. J., Chenery, S. R. N., Hamilton, E. M., Holdship, P., Peck, V. L., Poulton, A. J., Stinchcombe, M. C., and Wishner, K. F.: Planktic foraminifera iodine/calcium ratios from plankton tows, Front. Mar. Sci., 10, 1095570, https://doi.org/10.3389/fmars.2023.1095570, 2023.

Wong, G. T. F. and Zhang, L.: Changes in iodine speciation across coastal hydrographic fronts in southeastern United States continental shelf waters, Cont. Shelf Res., 12, 717–733, https://doi.org/10.1016/0278-4343(92)90027-H, 1992.

Zhou, X., Thomas, E., Rickaby, R. E. M., Winguth, A. M. E., and Lu, Z.: I/Ca evidence for upper ocean deoxygenation during the PETM, Paleoceanography, 29, 964–975, https://doi.org/10.1002/2014PA002702, 2014.

Zhou, X., Hess, A. V., Bu, K., Sagawa, T., and Rosenthal, Y.: Simultaneous Determination of I/Ca and Other Elemental Ratios in Foraminifera: Comparing Results From Acidic and Basic Solutions, Geochem. Geophy. Geosy., 23, e2022GC010660, https://doi.org/10.1029/2022GC010660, 2022.